Chapter 3
Multi-Valued Potentials in Topological Field Theory

Renzo L. Ricca, Matteo Foresti, and Xin Liu

Abstract In these lecture notes we review the original work of Riemann on multi-valued functions, Kelvin's application to Green's potential theory, and the result of Gauss on the interpretation of the magnetic potential in terms of solid angle to show the relevance of these earlier results in modern topological field theory. This is done by considering some particular case studies. First we re-derive the Biot-Savart induction law in terms of solid angle, and we discuss the interplay of topology and physics in the context of the celebrated Aharonov-Bohm experiment. By showing how the helicity is made gauge invariant in a multiply connected domain, we demonstrate how Riemann's cuts are re-interpreted in terms of modern homological concepts. Finally, by considering Kleinert's multi-valued gauge theory for defects we show how direct application of the theory of currents help to correct results in the hydrodynamic interpretation of vortex defects in condensed matter physics.

3.1 Riemann's Cuts and Multi-Valued Potentials

Once viewed as a mere mathematical artefact of physical theories, potential theory is now considered a fundamental tool to understand and describe subtle aspects of reality. With the recent advancements in topological field theory, and the study of knotted fields in particular, the role of multi-valued potentials in multiply connected

R. L. Ricca (✉) · M. Foresti
Department of Mathematics and Applications, University of Milano-Bicocca, Milan, Italy
e-mail: renzo.ricca@unimib.it

X. Liu
Institute of Theoretical Physics, Faculty of Sciences, Beijing University of Technology, Beijing, P.R. China

© The Author(s), under exclusive license to Springer Nature Switzerland AG 2024

R. L. Ricca, X. Liu (eds.), *Knotted Fields*, Lecture Notes in Mathematics 2344,
https://doi.org/10.1007/978-3-031-57985-1_3

domains has received new impetus. In this respect Riemann's foundational work published in his *"Propositions from analysis situs ..."* [26] provides still a perfect, elementary introduction to some fundamental concepts in topological field theory. It seems therefore quite appropriate to start these lecture notes from re-considering Riemann's paper, showing how his ideas provide inspiration for current research in the study of knotted fields.

Let us begin by considering the simple case of a two-dimensional, bounded region $R \subset \mathbb{R}^2$ of compact support, and assume R to be oriented according to the orientation of its boundary $\mathcal{C}_0 \equiv \partial R$. Let $u = u(x, y)$ and $v = v(x, y)$ be two continuous functions of the point coordinates in the plane (x, y). The differential form $u(x, y)\,\mathrm{d}x + v(x, y)\,\mathrm{d}y$ is said to be *exact* on R if there exists some differentiable scalar function $\phi = \phi(x, y)$ defined on R, such that

$$\mathrm{d}\phi = \frac{\partial \phi}{\partial x} dx + \frac{\partial \phi}{\partial y} \mathrm{d}y = u\,\mathrm{d}x + v\,\mathrm{d}y \tag{3.1}$$

throughout R. We assume that

$$\frac{\partial v}{\partial x} = \frac{\partial}{\partial x}\left(\frac{\partial \phi}{\partial y}\right) = \frac{\partial}{\partial y}\left(\frac{\partial \phi}{\partial x}\right) = \frac{\partial u}{\partial y}\,, \tag{3.2}$$

so that

$$\frac{\partial v}{\partial x} - \frac{\partial u}{\partial y} = 0\,. \tag{3.3}$$

If we regard the left-hand side of (3.3) as the z-component of the curl of a vector field in $\mathbb{R}^3$, we can immediately recognise the correspondence between the exactness of a differential form and the curl-free condition in $\mathbb{R}^3$. Now, let's go back to the two-dimensional case: by Stokes' theorem the form $d\phi$ can be integrated directly over the boundary $\mathcal{C}_0$, so that from (3.1) and (3.3) we have

$$\oint_{\mathcal{C}_0} (u\,\mathrm{d}x + v\,\mathrm{d}y) = \int_R \left(\frac{\partial v}{\partial x} - \frac{\partial u}{\partial y}\right) \mathrm{d}x\,\mathrm{d}y = 0\,. \tag{3.4}$$

If $\mathrm{d}\boldsymbol{l}$ represents an elementary displacement along a given path in $\mathbb{R}^2$, we can write $\mathrm{d}\phi = \boldsymbol{\nabla}\phi \cdot \mathrm{d}\boldsymbol{l}$, and use the gradient theorem to compute the line integral between two points P and Q in R; we have

$$I(P, Q) = \int_P^Q \mathrm{d}\phi = \int_P^Q \boldsymbol{\nabla}\phi \cdot \mathrm{d}\boldsymbol{l} = \phi(Q) - \phi(P)\,, \tag{3.5}$$

an established result for a *conservative* vector field $\boldsymbol{u} = (u, v) = \boldsymbol{\nabla}\phi$ in terms of the potential function ϕ.

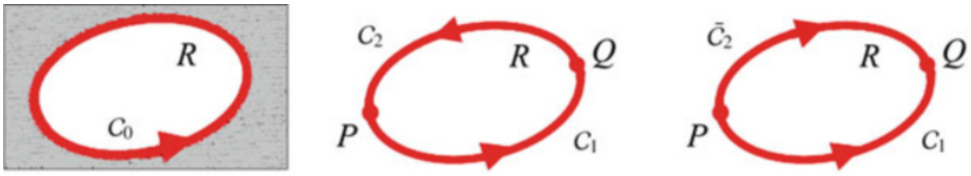

Fig. 3.1 (Left) Let R be a two-dimensional, simply connected region (white area) bounded by the oriented curve $\mathcal{C}_0 = \partial R$. (Centre) $\mathcal{C}_0$ can be decomposed into two consecutive, oriented arcs $\mathcal{C}_1$ and $\mathcal{C}_2$, with end points at P and Q. (Right) By reversing the orientation of $\mathcal{C}_2$ (thus obtaining the new oriented path $\bar{\mathcal{C}}_2$), we can go from P to Q either along $\mathcal{C}_1$ or $\bar{\mathcal{C}}_2$

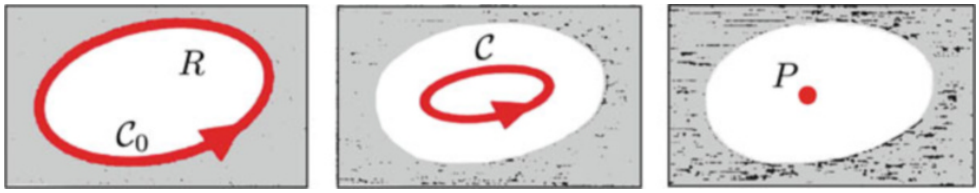

Fig. 3.2 (Left) If R (white area) is simply connected, then $\mathcal{C}_0$ can be continuously deformed through a sequence of arbitrary loops $\mathcal{C}$ (central panel) to a single point P in R

If the oriented path is given by a simple, closed curve (i.e. a loop with $P \equiv Q \in \mathcal{C}_0$), then $I(P, Q)$ is the circulation of $\boldsymbol{u}$ over $\mathcal{C}_0$:

$$\Gamma_{\mathcal{C}_0} = \oint_{\mathcal{C}_0} \mathrm{d}\phi = 0 \,. \tag{3.6}$$

In this case equation (3.5) can be proven directly and simply: consider $\mathcal{C}_0 = \mathcal{C}_1 \cup \mathcal{C}_2$ (see Fig. 3.1), where $\mathcal{C}_1$ and $\mathcal{C}_2$ are two consecutive arcs with end points at P and Q; by reversing the orientation (and parametrisation) of $\mathcal{C}_2$ to $\bar{\mathcal{C}}_2$ we can see that the line integrals over $\mathcal{C}_1$ and $\bar{\mathcal{C}}_2$ coincide; hence the integral $I(P, Q)$ is path-independent.

If R has no internal holes or obstacles, $\mathcal{C}_0$ can be continuously deformed to a single point in R by a sequence of arbitrary, intermediate, closed paths $\mathcal{C}$. So, any loop $\mathcal{C}$ (homotopic equivalent to $\mathcal{C}_0$) can be contracted to a point: the loop (or cycle) is said to be reducible (or *contractible*) in R (Fig. 3.2), and R is said to be *simply connected* in $\mathbb{R}^2$. Since equation (3.6) holds true for any point, and for any loop in R, we have

$$\Gamma_{\mathcal{C}} = \oint_{\mathcal{C}} \mathrm{d}\phi = 0 \qquad \forall \mathcal{C} \subset R \,, \tag{3.7}$$

which is a property of the simply connected region R. Moreover, if $\boldsymbol{u} = \nabla\phi$ is also solenoidal on R (i.e. $\nabla \cdot \boldsymbol{u} = 0$), we have that $\nabla \cdot \nabla\phi = \nabla^2\phi = 0$: in simply connected domains solenoidal vector fields can be defined in terms of harmonic potentials. Remember that while conservative vector fields are irrotational by definition (i.e. regardless of the connectivity of the domain), irrotational fields are conservative only if the domain of definition is simply connected.

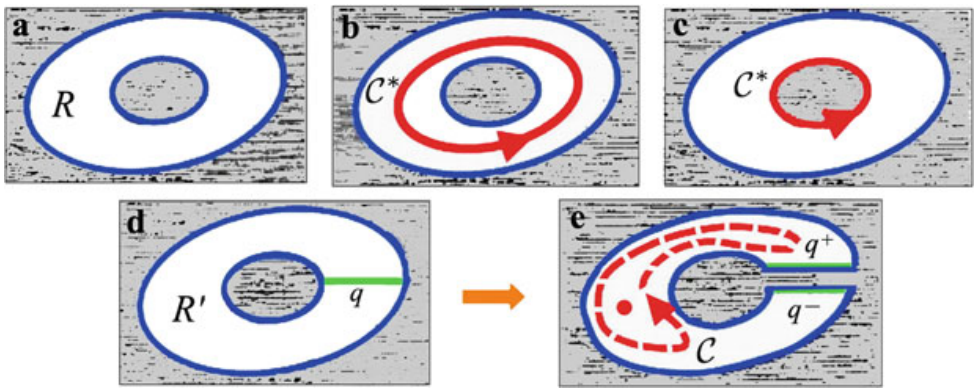

Fig. 3.3 (**a**)–(**c**). In a doubly connected region R (white area) the presence of an obstruction (represented by the grey patch in the interior) prevents the loop $\mathcal{C}^*$ to be reduced to a point. (**d**)–(**e**) The region R can be reduced to a simply connected region R' by inserting a cut q so that any loop $\mathcal{C}$ in R' can be reduced to a point. (**e**) The presence of the cut is emphasised by showing the presence of the new boundary arcs q^- and q^+

Now, let us consider the region shown in Fig. 3.3a, where an obstruction represented by the grey patch is present in the interior. Evidently there is at least one loop $\mathcal{C}^*$ embracing this obstruction (panel b) that cannot be reduced to a point (panel c). Since $\mathcal{C}^*$ is non-reducible, the integral (3.7) over $\Gamma_{\mathcal{C}^*}$ does not vanish. If the line integral is computed by polar coordinates the result is expressed by a multi-valued function, because of the multi-valued periodicity of the polar angle; hence, assuming positive circulation, we obtain $\Gamma_{\mathcal{C}^*} = 2\pi n$ ($n \in \mathbb{N}$). As proposed by Riemann, we can restore simple connectivity by inserting a number of *cuts*. In the particular case of Fig. 3.3 such a procedure is achieved by the insertion of a single cut q (panel d), that goes from a point of the inner boundary to another point of the outer boundary of R. As emphasised by panel (e), the new region R' is now simply connected, so that any loop in R' can be reduced to a point; note that the insertion of the cut modifies the original boundary of R by the additional boundary arcs q^- and q^+ (the two sides of the cut). In Riemann's own words, we have:

Definition 3.1 By means of a cut, any $(n + 1)$-ply connected region R can be reduced to an n-ply connected region R'. The boundary arcs resulting from a cut form a new boundary, for a cut cannot pass through any point more than once, but it can end at one of its earlier points.

This definition can be extended to compact, orientable, two-dimensional surfaces S, distinguished in simply connected surfaces, and *multiply connected* surfaces, where one can find at least one, non-reducible loop. According to Riemann, we have:

Definition 3.2 A surface S is said to be $(n + 1)$-ply connected, when n loops can be drawn on it, so that neither individually, nor in combination bound a region of S, whereas if augmented by any other loop the set of loops bounds some region of S.

In Riemann's words such surfaces are defined by "the maximum number n of cuts [given by non-intersecting cycles] that can be performed on S, without making S disconnected". We have:

Theorem 3.1 (Riemann, 1857) *An $(n+1)$-ply connected surface S is changed into an n-ply connected surface S' by a cut that does not disconnect the original surface S.*

If S is the domain of definition of a potential function one can regard the obstructions present in S as holes, and since there is a one-to-one correspondence between the number n of cuts necessary to reduce the domain to simple connectivity, and the number g of holes present in S, we can denote the multiple connectivity of S by the number of holes, that defines the *genus* g of S. Any multiply connected surface can thus be reduced to a simply connected one by inserting $n = g$ cuts, as additional boundary surfaces of the simply connected surface. If one deals with closed surfaces, g can also be defined in terms of the Euler characteristic χ by the formula $2g = 2 - \chi$; if such surfaces have b boundary components, we have $2g = 2 - b - \chi$. In a three-dimensional handle-body representation of a closed surface (no boundary), g represents the number of holes (or handles) present in S, and it is often referred to as the (first) *Betti number* of S. Evidently g denotes the maximum number of cuts of embedded disks that do not make the resultant manifold disconnected into separate parts. Two examples of triply connected surfaces are given by the doubly covered surface of Fig. 3.4, or by the 2-hole doughnut of Fig. 3.14.

If S covers the (xy)-plane with two overlapped sheets (as shown in Fig. 3.4) we reduce the surface to a simply connected one by inserting two cuts: the cut q_1, that can be identified with the arc of end points α, β, and the cut q_2 of end points γ, δ. Ideally we can regard the two sheets delimited by α, β, γ, δ as *branches* of a multi-covered, layered surface that depart from each inserted cut. The new, multi-branched surface S' is now a simply connected surface. The *branch points* are thus the loci where the multiple layers meet. Any function $I = I(P, Q)$ originally defined on

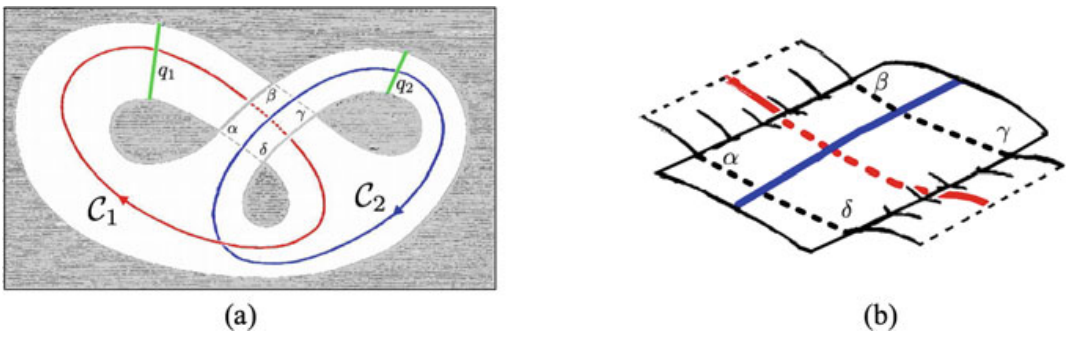

Fig. 3.4 (**a**) Riemann's example of a doubly covered, triply connected surface S, where $\mathcal{C}_1$ and $\mathcal{C}_2$ denote two non-reducible cycles (drawings adapted from [26]); S becomes a simply connected surface S' by inserting the two cuts q_1 and q_2. (**b**) The region delimited by $\alpha, \beta, \gamma, \delta$ is doubly covered by the two sheets of S

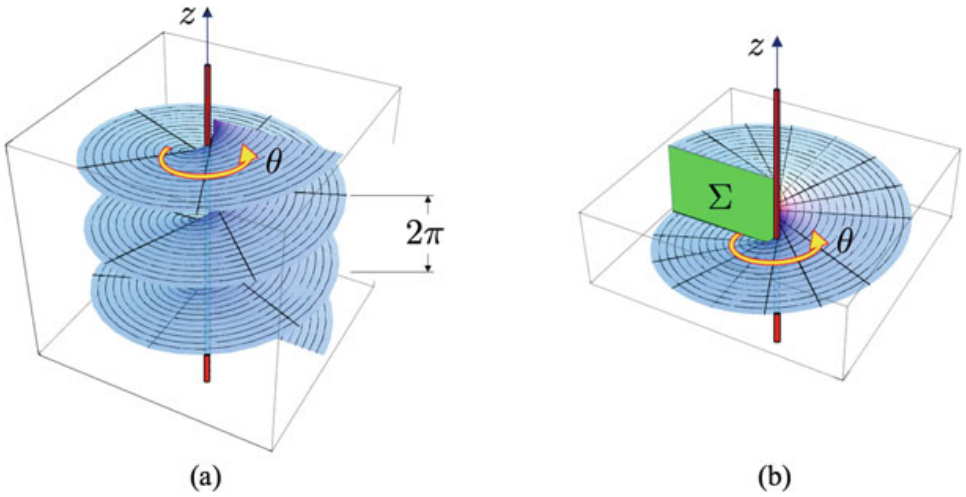

Fig. 3.5 (**a**) Three-dimensional representation of the multi-valued, real function $\theta = \tan^{-1}(y/x)$ mod 2π. The periodicity of the function is visualised by infinitely many copies of sheets. The central, thin tube (along the z-axis) emphasises the location of the essential singularity associated with the pole of the function. (**b**) The standard way to make the function single-valued is to restrict the domain of definition by inserting a "branch" cut Σ

S results then well-defined on S', because by analytical continuation through the branch points the integral $I = I(P, Q)$ results continuous, and uniquely determined at every point of S' [2]. Technically speaking, Riemann's ingenious idea to replace multiply connected surfaces with multi-branched, simply connected ones is rooted in his work on multi-valued, holomorphic functions of a complex variable z, but it can equally be applied to the case of ordinary, multi-valued, real functions (see Fig. 3.5). For a modern introduction to topology the interested reader can consult, for example, [18].

3.2 Kelvin's Application of Riemann's Cuts

In developing his vortex atom theory [28], Kelvin proposed as fundamental constituents of matter knotted vortices embedded in a hypothetical microcosm (the so-called *æther*) made of an ideal, irrotational fluid. Since in ideal conditions rotational and irrotational regions do not mix (that is a consequence of Helmholtz's conservation laws [16]), from a kinetic potential theory viewpoint such vortices represent tubular holes in an irrotational medium (see Fig. 3.6). For the irrotational kinetic potential these vortices are like holes (i.e. empty tunnels), that make the irrotational fluid a multiply connected region. Kelvin notices that in this context Green's first identity needs a correction [3], and addresses the question by considering a particular example to understand the mathematical properties of a multiply connected fluid æther.

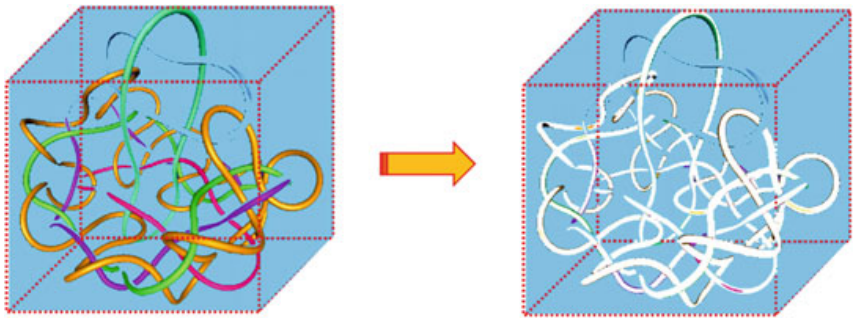

Fig. 3.6 Knotted vortices in an ideal, irrotational fluid. For the kinetic potential of an irrotational flow the vortex tubes are like holes represented by empty tunnels

3.2.1 Kelvin's Case Study

In Sec. 56 of his 1869 paper, Kelvin [28] considers the case of an ideal, incompressible fluid in a region $D \subset \mathbb{R}^3$ of compact support and volume V, defined by a portion of a circular cylinder, centred on the z-axis, and bored along its axis by a tubular, empty region, where an irrotational kinetic potential is defined. The cylinder is limited by the planes $z = z_0$ and $z = z_1$, and is defined by an outer radius r_1 and an inner radius $r_0 < r_1$. Since the system is axially symmetric about the z-axis, we can consider the motion of a fluid around the z-axis given by a two-dimensional flow in the azimuthal direction in an annulus of the (xy)-plane (see Fig. 3.7a). The kinetic potential associated with the velocity $\boldsymbol{u} = \nabla\psi$, is given by the scalar function

$$\psi(x, y) = \tan^{-1}\left(\frac{y}{x}\right), \tag{3.8}$$

and this ψ can be identified with the polar coordinate θ. Fluid motion is thus governed by the following equations:

$$\frac{\partial\psi}{\partial x} = \frac{-y}{x^2 + y^2}, \qquad \frac{\partial\psi}{\partial y} = \frac{x}{x^2 + y^2},$$

with

$$\boldsymbol{u}(x, y) = \left(\frac{-y}{x^2 + y^2}, \frac{x}{x^2 + y^2}\right). \tag{3.9}$$

We can easily verify that $\boldsymbol{u}$ is solenoidal and irrotational in the xy-plane, i.e.

$$\nabla^2\psi = \frac{\partial^2\psi}{\partial x^2} + \frac{\partial^2\psi}{\partial y^2} = 0\,. \tag{3.10}$$

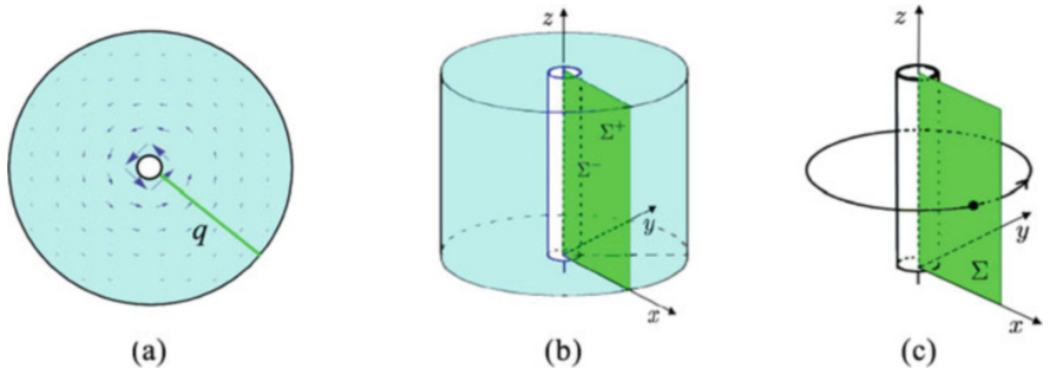

Fig. 3.7 (**a**) Cross-section of the doubly-connected region D; simple connectivity is restored by inserting the cut q. (**b**) In three dimensions the cut is represented by the surface Σ. (**c**) This surface can be viewed as a "barrier stopping circulation" around the z-axis

Let $S = \partial D$ be the bounding surface of D, with outward unit normal $\hat{\boldsymbol{v}}$. By application of the divergence theorem, we have

$$\int_V \nabla \cdot \boldsymbol{u}\, \mathrm{d}V = \int_S \boldsymbol{u} \cdot \mathrm{d}\boldsymbol{S}\,, \tag{3.11}$$

where $\mathrm{d}\boldsymbol{S} = \mathrm{d}S\,\hat{\boldsymbol{v}}$. A velocity field can be defined in full generality by two potentials ϕ and ψ by taking $\boldsymbol{u} = \phi\,\nabla\psi$, where $\phi = \phi(\boldsymbol{x})$ and $\psi = \psi(\boldsymbol{x})$ are two, sufficiently smooth scalar functions of the vector position $\boldsymbol{x} \in D$. By substituting these expressions into (3.11), we have

$$\int_V \nabla \cdot (\phi\,\nabla\psi)\mathrm{d}V = \int_S \phi\,\nabla\psi \cdot \mathrm{d}\boldsymbol{S}\,, \tag{3.12}$$

which gives *Green's first identity* in the form

$$\int_V \left(\nabla\phi \cdot \nabla\psi + \phi\nabla^2\psi\right)\mathrm{d}V = \int_S \phi\,\nabla_{\hat{\boldsymbol{v}}}\psi\,\mathrm{d}S\,, \tag{3.13}$$

where $\nabla_{\hat{\boldsymbol{v}}}\psi$ denotes the directional derivative of ψ along $\hat{\boldsymbol{v}}$. Let us re-write equation (3.13) in the two equivalent, alternative forms, given by

$$\int_V \nabla\phi \cdot \nabla\psi\,\mathrm{d}V = -\int_V \phi\nabla^2\psi\,\mathrm{d}V + \int_S \phi\nabla_{\hat{\boldsymbol{v}}}\psi\,\mathrm{d}S\,. \tag{3.14}$$

and

$$\int_V \nabla\phi \cdot \nabla\psi\,\mathrm{d}V = -\int_V \psi\nabla^2\phi\,\mathrm{d}V + \int_S \psi\nabla_{\hat{\boldsymbol{v}}}\phi\,\mathrm{d}S\,, \tag{3.15}$$

Assuming ϕ to be single-valued, Eq. (3.14) holds true even if ψ is multi-valued, because the gradient of a multi-valued function is anyway single-valued. This is not so for Eq. (3.15), where the multi-valuedness of ψ introduces an arbitrariness in the integrals on the right-hand side.

To see this in detail, let us first evaluate the integral contributions in Eq. (3.14). With reference to Fig. 3.7, and using cylindrical polar coordinates (r, θ, z) centred on z, let us compute $\nabla_{\hat{\mathfrak{v}}}\psi$ in the last integral on the right-hand side of (3.14). Because $\boldsymbol{u}$ is two-dimensional, there is no flux of $\boldsymbol{u}$ through the annular surfaces at $z = z_0$ and $z = z_1$; moreover, since $\psi = \tan^{-1}(y/x) \equiv \theta$, we have $\nabla_{\hat{\mathfrak{v}}}\psi = \nabla_{\hat{\boldsymbol{e}}_r}\theta$ in the radial direction, so that

$$\nabla_{\hat{\mathfrak{v}}}\psi = \Big[\Big(\frac{\partial}{\partial r}\hat{\boldsymbol{e}}_r + \frac{1}{r}\frac{\partial}{\partial\theta}\hat{\boldsymbol{e}}_\theta + \frac{\partial}{\partial z}\hat{\boldsymbol{e}}_z\Big)\theta\Big]\cdot\hat{\boldsymbol{e}}_r = \frac{1}{r}\,\hat{\boldsymbol{e}}_\theta\cdot\hat{\boldsymbol{e}}_r = 0\,; \tag{3.16}$$

hence, because of (3.10) and (3.16) both integrals on the right-hand side of (3.14) vanish. On the other hand direct computation of the integral on the left-hand side of (3.14) gives

$$I_1 = \int_V \nabla\phi\cdot\nabla\psi\,\mathrm{d}V = \int \frac{x\partial_y\phi - y\partial_x\phi}{x^2+y^2}\,\mathrm{d}x\,\mathrm{d}y\,\mathrm{d}z\,; \tag{3.17}$$

since the integrand in cylindrical coordinates becomes

$$\frac{x\partial_y\phi - y\partial_x\phi}{x^2+y^2} = \frac{1}{r^2}\frac{\partial\phi}{\partial\theta}\,,$$

application of the gradient theorem gives

$$I_1 = \int \frac{1}{r^2}\frac{\partial\phi}{\partial\theta}\,\mathrm{d}r\,r\mathrm{d}\theta\,\mathrm{d}z = \int_{z_0}^{z_1}\mathrm{d}z\int_{r_0}^{r_1}\frac{1}{r}\,\mathrm{d}r\int_0^{2\pi}\frac{\partial\phi}{\partial\theta}\,\mathrm{d}\theta = 0\,. \tag{3.18}$$

Hence, by substituting (3.10), (3.16) and (3.18) into (3.14), Green's first identity in that form results satisfied.

Let us consider now Green's first identity in the form given by Eq. (3.15). Since ψ is multi-valued, there is no guarantee that that equality holds. The integral on the left-hand side is still zero, but there is no guarantee that the term on the right-hand side remains zero, because the ψ-values are now only determined up to mod 2π, so that we can only state that

$$-\int_V \tan^{-1}\Big(\frac{y}{x}\Big)\nabla^2\phi\,\mathrm{d}V + \int_S \tan^{-1}\Big(\frac{y}{x}\Big)\nabla_{\hat{\mathfrak{v}}}\phi\,\mathrm{d}S \neq 0\,. \tag{3.19}$$

In order to remove this ambiguity, we must restore simple connectivity by making the right-hand side well-defined. As Kelvin noticed, according to Riemann's theory

this can be done by inserting a cut in the (xz)-plane given by the surface Σ, thus reducing D to simple connectivity (Fig. 3.7b). Noting that the presence of Σ does not alter the volume V, its presence changes the boundary S, changing the surface integral in (3.19). By considering the two sides of Σ, the new boundary S' is modified by the presence of the two contributions Σ^- and Σ^+ of unit normal along $\hat{\boldsymbol{j}}$; since $S' \equiv S \cup \Sigma^- \cup \Sigma^+$, we must also take into account the two contributions of $\tan^{-1}(y/x)$ at Σ^- and Σ^+; we have $\tan^{-1}(y/x)|_{\Sigma^-} = \theta|_{\Sigma^-} = 0$, and $\tan^{-1}(y/x)|_{\Sigma^+} = \theta|_{\Sigma^+} = 2\pi$, so that Eq. (3.19) is no longer arbitrary; hence, using (3.18) we can definitely write

$$-\int_V \tan^{-1}\left(\frac{y}{x}\right)\nabla^2\phi\,\mathrm{d}V + \int_S \tan^{-1}\left(\frac{y}{x}\right)\nabla_{\hat{\boldsymbol{\nu}}}\phi\,\mathrm{d}S + 2\pi\int_{\Sigma^+}\nabla_{\hat{\boldsymbol{j}}}\,\phi\big|_{y=0}\,\mathrm{d}x\mathrm{d}z = 0\,, \tag{3.20}$$

where the function $\tan^{-1}(y/x)$ is single-valued in the new domain of definition. By re-writing Eq. (3.20) in the standard form of the divergence theorem, we have

$$\int_V \tan^{-1}\left(\frac{y}{x}\right)\nabla^2\phi\,\mathrm{d}V = \int_S \tan^{-1}\left(\frac{y}{x}\right)\nabla_{\hat{\boldsymbol{\nu}}}\phi\,\mathrm{d}S + 2\pi\int_{\Sigma^+}\nabla_{\hat{\boldsymbol{j}}}\,\phi\big|_{y=0}\,\mathrm{d}x\mathrm{d}z\,, \tag{3.21}$$

where each term above is well-defined and continuous. Since the value of 2π results from the computation of ψ on the opposite sides of Σ, we can write

$$2\pi = [\psi]_{\Sigma^-}^{\Sigma^+} = \oint_{\mathcal{C}_0}\nabla\psi\cdot\mathrm{d}\boldsymbol{l} = \kappa\,, \tag{3.22}$$

where $\mathcal{C}_0$ denotes a simple loop around the central hole, and $\mathrm{d}\boldsymbol{l} = \mathrm{d}l\,\hat{\boldsymbol{t}}$ ($\hat{\boldsymbol{t}}$ unit tangent to $\mathcal{C}_0$). The circulatory constant κ is associated with the cut surface Σ, viewed in Kelvin's own words as a "circulation stopping barrier" (see Fig. 3.7c).

3.2.2 *Kelvin's Correction to Green's First Identity*

Kelvin's case study provides the correction to Green's first identity in the presence of a multiply connected domain $\mathcal{M}$. As the number of cuts/loops corresponds to the (first) Betti number g of holes present on $\mathcal{M}$, reduction to simple connectivity by $n = g$ cuts/loops modifies the boundary of $\mathcal{M}$ by a number g of Σ_i $(i = 1, \ldots, g)$ surfaces. In more modern words Kelvin's result ([28], Sec. 57) can thus be stated as follows:

Lemma 3.1 (Thomson, 1869) *A multiply connected, compact manifold $\mathcal{M}$ of Betti number g, volume V, and boundary surface S, is reduced to simple connectivity by the insertion of g cut surfaces Σ_i $(i = 1, \ldots, g)$, so that Green's first identity for*

the multi-valued potential ψ associated with the field $\boldsymbol{u} = \phi\nabla\psi$ on $\mathcal{M}$ becomes

$$\int_V \left(\nabla\psi \cdot \nabla\phi + \psi\nabla^2\phi\right)\mathrm{d}V = \int_S \psi\nabla_{\hat{\mathfrak{v}}}\phi\,\mathrm{d}S + \sum_{i=1}^{g}\kappa_i \int_{\Sigma_i} \nabla_{\hat{\mathfrak{v}}}\phi\,\mathrm{d}S\,, \tag{3.23}$$

where κ_i denotes the circulatory constant associated with Σ_i.

Since κ_i is due to the circulation of a potential function, it represents the *potential strength* of each hole, providing a quantitative information for each hole on $\mathcal{M}$.

3.3 Gauss' Solid Angle Interpretation of the Potential

The use of multi-valued scalar potentials has an interesting, alternative application by considering an example that comes from Gauss' original work on geomagnetism [15, 25]. Gauss derives his theory from first principles, defining the scalar potential $\mathscr{V} = \mathscr{V}(P)$ at a point P associated with a hypothetical magnetic shell of strength I in terms of the solid angle subtended by the shell at P. The magnetic shell is given by a surface S, whose opposite sides S^- and S^+ are assumed to have opposite polarity (see Fig. 3.8a). As reported by Kelvin [27], Gauss states the following result:

Theorem 3.2 (Gauss [15]) *The potential $\mathscr{V}$ of a magnetic shell S of strength I at any point P in space is equal to the solid angle Ω which it subtends at that point multiplied by its magnetic strength I.*

The theorem is derived from geometric considerations of certain elementary expressions of potential theory. Since the induced potential at P is given by the amount of the field of view spanned by S from the observation point P, it is measured by the solid angle Ω that S subtends at P (Fig. 3.8a). This solid angle is given by the projection of S onto the unit sphere with centre at P, and in spherical coordinates

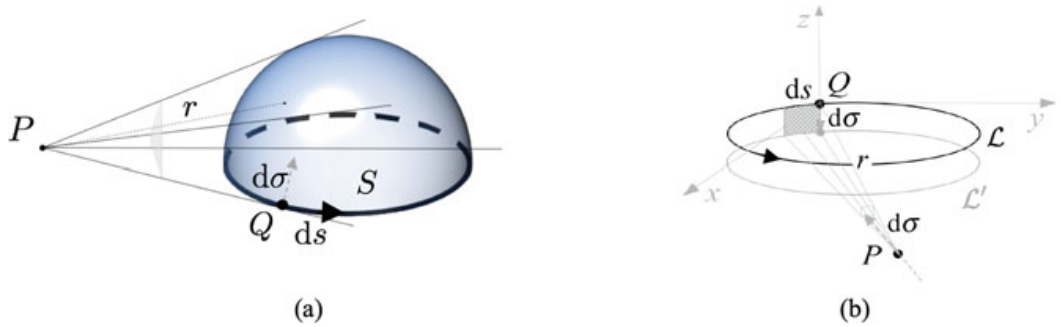

Fig. 3.8 (**a**) The potential $\mathscr{V}$ at a point P, due to a magnetised hemispherical shell of surface S and boundary $\mathcal{L} = \partial S$, is given by the solid angle subtended by S at P. (**b**) Maxwell's interpretation of the solid angle in terms of the apparent displacement of a current carrying loop $\mathcal{L}$ observed when a magnetic pole moves from infinity to the position at P

it is standardly defined in terms of the polar angle (colatitude) $\theta \in [0, \pi]$ and the azimuth angle (longitude) $\varphi \in [0, 2\pi]$ by

$$\Omega = \int \mathrm{d}\varpi = \iint \sin\theta \, \mathrm{d}\theta \, \mathrm{d}\varphi \, . \tag{3.24}$$

In the present case the elementary solid angle $\mathrm{d}\varpi$ is given by the volume of the pyramid of base $\mathrm{d}S = \mathrm{d}s \, \mathrm{d}\sigma$ (s and σ being two surface coordinates), side r, and apex at P:

$$\frac{1}{3} r^3 \mathrm{d}\varpi = \frac{1}{3} r^3 \Pi \, \mathrm{d}s \mathrm{d}\sigma \, , \tag{3.25}$$

where $r = |\boldsymbol{x} - \boldsymbol{x}^*|$ is the distance between $P = P(\boldsymbol{x})$ and the source point $Q = Q(\boldsymbol{x}^*) \in S$; Π is a quantity (to be determined) of dimension L^{-2}. The resulting potential $\mathscr{V}$ is thus given by the solid angle

$$\Omega(\boldsymbol{x}) = \iint \Pi \, \mathrm{d}s \, \mathrm{d}\sigma \, . \tag{3.26}$$

To compute Π, Gauss uses a fundamental result due to Ampère (see again [27]):

Theorem 3.3 (Ampère, 1831) *A closed electric circuit $\mathcal{L}$ produces the same effect as a magnetic shell S of any form having the circuit $\mathcal{L}$ for its edge.*

By identifying the boundary curve ∂S with a current carrying loop $\mathcal{L}$ of same strength I, and noticing that the potential is a symmetric function of P and Q, Maxwell ([21], Sec. 419) provides an interpretation of the magnetic potential as the work done by a magnetic pole, when this pole is brought from infinity (where the potential is zero) to the position at P. According to Maxwell the double integration in $\mathrm{d}s \, \mathrm{d}\sigma$ can be interpreted in terms of the apparent displacement of $\mathcal{L}$ (of arc-length s) envisaged when the pole travels from infinity to P along a path γ of arc-length σ (see Fig. 3.8b). The contribution to the solid angle, computed in terms of direction cosines, is given by

$$\Pi = \frac{1}{r^3} \det \begin{pmatrix} x - x^* & y - y^* & z - z^* \\ \dfrac{\mathrm{d}x}{\mathrm{d}s} & \dfrac{\mathrm{d}y}{\mathrm{d}s} & \dfrac{\mathrm{d}z}{\mathrm{d}s} \\ \dfrac{\mathrm{d}x^*}{\mathrm{d}\sigma} & \dfrac{\mathrm{d}y^*}{\mathrm{d}\sigma} & \dfrac{\mathrm{d}z^*}{\mathrm{d}\sigma} \end{pmatrix} \, , \tag{3.27}$$

so that the potential $\mathscr{V}$ in terms of the solid angle is given by

$$\mathscr{V} = \oint_{\mathcal{L}} \int_{\gamma} \Pi \, \mathrm{d}s \, \mathrm{d}\sigma = \int_S \frac{\hat{\boldsymbol{r}} \cdot \mathrm{d}\boldsymbol{S}}{r^2} \, , \tag{3.28}$$

where $\hat{\boldsymbol{r}} = (\boldsymbol{x} - \boldsymbol{x}^*)/|\boldsymbol{x} - \boldsymbol{x}^*|$.

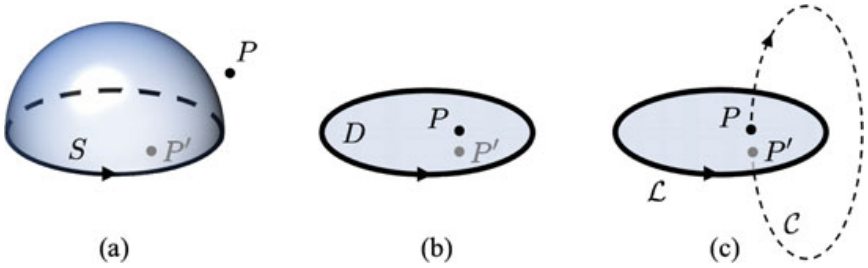

Fig. 3.9 (**a**) By Ampère's theorem the induction at P due to a magnetised shell of surface S and boundary $\mathcal{L} = \partial S$ is (**b**) equivalent to the induction at P of a disc D with the same boundary $\mathcal{L}$ of S; (**c**) when P goes from a position infinitely close to the positive side of D to its antipodal position at P' on the opposite side of D, the value of the solid angle jumps by 4π

Note that when P goes from a position infinitely near S^+ to a position infinitely near S^-, without going through S, the value of the solid angle changes by 4π. We can see this in 3 steps: first, by using Ampère's theorem, deform S to a planar disc D (see Fig. 3.9a, b); then place P infinitely near D^+, so that the solid angle is half of the surface area of a unit sphere (i.e. $\Omega = +2\pi$); finally, move P to its antipodal position P' near D^-, so that $\Omega = -2\pi$, with the jump $[\Omega] = 4\pi$. In Kelvin's words, we have

Corollary 3.1 (Thomson [27]) *Of two points infinitely near one another on the two sides of a magnetic shell, but not infinitely near its edge, the potential at that one which is on the north polar side exceeds the potential at the other by the constant* 4π.

As Maxwell pointed out, when P moves along a path $\mathcal{C}$ that embraces the loop $\mathcal{L}$ simply (see Fig. 3.9c), the solid angle gives information on the linking number between $\mathcal{C}$ and $\mathcal{L}$ (see Sect. 3.3.2 below).

3.3.1 Interpretation of the Biot-Savart Law in Terms of Solid Angle

The Biot-Savart law that prescribes the effect of a source field (placed at $\boldsymbol{x}^*$) at a point $\boldsymbol{x}$ can be expressed in terms of solid angle [17, Problem 5.1, p. 225]. To see this, consider a current carrying wire loop $\mathcal{L}$ of infinitesimal cross-section, and strength I (for simplicity we set magnetic permeability to one). If $\boldsymbol{x}^* \in \mathcal{L}$ we can write the Biot-Savart law as a line integral, given by

$$\begin{aligned}\boldsymbol{B}(\boldsymbol{x}) =& \frac{I}{4\pi}\oint_{\mathcal{L}} \frac{\mathrm{d}\boldsymbol{l}\times(\boldsymbol{x}-\boldsymbol{x}^*)}{|\boldsymbol{x}-\boldsymbol{x}^*|^3} = -\frac{I}{4\pi}\oint_{\mathcal{L}} \mathrm{d}\boldsymbol{l}\times\nabla\frac{1}{|\boldsymbol{x}-\boldsymbol{x}^*|}\\ =& \frac{I}{4\pi}\nabla\times\oint_{\mathcal{L}}\frac{\mathrm{d}\boldsymbol{l}}{|\boldsymbol{x}-\boldsymbol{x}^*|} = \frac{I}{4\pi}\nabla\times\boldsymbol{A}(\boldsymbol{x})\,,\end{aligned} \tag{3.29}$$

where $\mathrm{d}\boldsymbol{l} = \mathrm{d}\boldsymbol{l}(\boldsymbol{x})$ is a line element of $\mathcal{L}$; ∇ operates on $\boldsymbol{x}$, and $\boldsymbol{A} = \boldsymbol{A}(\boldsymbol{x})$, defined by the last equality, is a vector potential. Take a unit vector $\hat{\boldsymbol{e}}$ fixed in space, and define the scalar quantity

$$A_{\mathrm{e}} = \boldsymbol{A} \cdot \hat{\boldsymbol{e}} = \oint_{\mathcal{L}} \frac{\mathrm{d}\boldsymbol{l} \cdot \hat{\boldsymbol{e}}}{|\boldsymbol{x} - \boldsymbol{x}^*|} \,. \tag{3.30}$$

If we apply Stokes' theorem to the line integral above, we have

$$A_{\mathrm{e}} = \int_S \left(\nabla^* \times \frac{\hat{\boldsymbol{e}}}{|\boldsymbol{x} - \boldsymbol{x}^*|} \right) \cdot \mathrm{d}\boldsymbol{S} = \int_S \left(\mathrm{d}\boldsymbol{S} \times \nabla^* \frac{1}{|\boldsymbol{x} - \boldsymbol{x}^*|} \right) \cdot \hat{\boldsymbol{e}} \,, \tag{3.31}$$

where ∇^* operates on $\boldsymbol{x}^*$, and $\boldsymbol{S} = S\hat{\boldsymbol{v}}$ denotes the surface bounded by $\mathcal{L}$ of unit normal $\hat{\boldsymbol{v}}$, defined according to the right-hand rule given by the direction of the current. Noting that $\nabla^* f(\boldsymbol{x} - \boldsymbol{x}^*) = -\nabla f(\boldsymbol{x} - \boldsymbol{x}^*)$, Eq. (3.31) becomes

$$\boldsymbol{A}(\boldsymbol{x}) = \nabla \times \int_S \frac{\mathrm{d}\boldsymbol{S}}{|\boldsymbol{x} - \boldsymbol{x}^*|} = \nabla \times \boldsymbol{W}(\boldsymbol{x}) \,, \tag{3.32}$$

where $\boldsymbol{W} = \boldsymbol{W}(\boldsymbol{x})$ is defined by the last equality. Hence, from (3.29) we have

$$\boldsymbol{B}(\boldsymbol{x}) = \frac{I}{4\pi} \nabla \times [\nabla \times \boldsymbol{W}(\boldsymbol{x})] \,. \tag{3.33}$$

Using a standard vector identity, and Green's fundamental solution to the Poisson equation for $\boldsymbol{W}$, we have

$$\begin{aligned} \nabla \times (\nabla \times \boldsymbol{W}) = \nabla(\nabla \cdot \boldsymbol{W}) - \nabla^2 \boldsymbol{W} &= \nabla \int_S \nabla \cdot \frac{\mathrm{d}\boldsymbol{S}}{|\boldsymbol{x} - \boldsymbol{x}^*|} + 4\pi \int_S \delta(\boldsymbol{x} - \boldsymbol{x}^*)\, \mathrm{d}\boldsymbol{S} \\ &= -\nabla \int_S \frac{(\boldsymbol{x} - \boldsymbol{x}^*) \cdot \mathrm{d}\boldsymbol{S}}{|\boldsymbol{x} - \boldsymbol{x}^*|^3} + 4\pi \int_S \delta(\boldsymbol{x} - \boldsymbol{x}^*)\, \mathrm{d}\boldsymbol{S} = \nabla \Omega(\boldsymbol{x}) \,, \end{aligned} \tag{3.34}$$

where we used Eq. (3.28); the last integral vanishes because we assume $\boldsymbol{x}^* \neq \boldsymbol{x}$ (to avoid singularities). Thus, we have

$$\boldsymbol{B}(\boldsymbol{x}) = \frac{I}{4\pi} \nabla \Omega(\boldsymbol{x}) \,, \tag{3.35}$$

which expresses the magnetic field in terms of the magnetic potential given by the solid angle (3.28).

3.3.2 *Emergence of Topological Linking*

Considering the discussion of the example of Fig. 3.9c, combined with the results of Sect. 3.3.1, we see that the linking number concept emerges naturally from the law of induction of a current carrying wire $\mathcal{L}$ of strength I. Here, relying on the interpretation of the Biot-Savart law in terms of solid angle, we show that there is a direct connection between the solid angle concept and the linking number formula. To see this consider the current density given by $\boldsymbol{J} = \nabla \times \boldsymbol{B}$ (taking physical constants equal to 1), where $\boldsymbol{B}$ denotes the magnetic field generated by the current. Take a mathematical loop $\mathcal{C}$ that embraces $\mathcal{L}$ simply, and S the mathematical surface bounded by $\mathcal{C}$. Suppose that $\mathcal{L}$ pierces S at a single, isolated point (see Fig. 3.10a). The electric current I is the flux of $\boldsymbol{J}$ through S, so that by using Ampère's law and Stokes' theorem, we have

$$I = \int_S \boldsymbol{J} \cdot \mathrm{d}\boldsymbol{S} = \int_S \nabla \times \boldsymbol{B} \cdot \mathrm{d}\boldsymbol{S} = \oint_{\mathcal{C}} \boldsymbol{B} \cdot \mathrm{d}\boldsymbol{l} \,, \tag{3.36}$$

where $\mathrm{d}\boldsymbol{l} = \mathrm{d}\boldsymbol{l}(\boldsymbol{x})$ is a line element of $\mathcal{C}$. Suppose now that $\mathcal{L}$ winds around $\mathcal{C}$ a multiple number of times m (see Fig. 3.10b); in this case the total flux of $\boldsymbol{J}$ through S is given by m times the intensity I. Assuming that $\boldsymbol{J}$ is parallel to the unit normal $\hat{\boldsymbol{v}}$ to S, oriented according to the right-hand rule associated with the current direction, the total contribution to the circulation of $\boldsymbol{B}$ is given by

$$\int_S \boldsymbol{J} \cdot \mathrm{d}\boldsymbol{S} = \oint_{\mathcal{C}} \boldsymbol{B} \cdot \mathrm{d}\boldsymbol{l} = mI \qquad (m \in \mathbb{Z}) \,. \tag{3.37}$$

The field $\boldsymbol{B}$ at $\boldsymbol{x}$ is given by the Biot-Savart law (3.29), i.e.

$$\boldsymbol{B}(\boldsymbol{x}) = \frac{I}{4\pi} \oint_{\mathcal{L}} \frac{\mathrm{d}\boldsymbol{l}(\boldsymbol{x}^*) \times (\boldsymbol{x} - \boldsymbol{x}^*)}{|\boldsymbol{x} - \boldsymbol{x}^*|^3} \,, \tag{3.38}$$

where $\mathrm{d}\boldsymbol{l}(\boldsymbol{x}^*)$ is a line element of $\mathcal{L}$. If $\mathcal{L}$ goes m times through S, by using (3.38) we have the total flux through $\mathcal{C}$; this is given by

$$\int_S \boldsymbol{J} \cdot \mathrm{d}\boldsymbol{S} = \oint_{\mathcal{C}} \boldsymbol{B} \cdot \mathrm{d}\boldsymbol{l} = \frac{I}{4\pi} \oint_{\mathcal{C}} \oint_{\mathcal{L}} \frac{\mathrm{d}\boldsymbol{l}(\boldsymbol{x}^*) \times (\boldsymbol{x} - \boldsymbol{x}^*) \cdot \mathrm{d}\boldsymbol{l}(\boldsymbol{x})}{|\boldsymbol{x} - \boldsymbol{x}^*|^3} = mI \,, \tag{3.39}$$

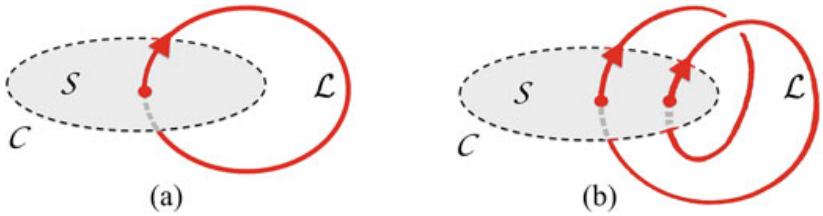

Fig. 3.10 (**a**) A mathematical loop $\mathcal{C}$, which bounds the surface S, embraces a current carrying loop $\mathcal{L}$; (**b**) if the wire forms m coils, the surface S is pierced m times by $\mathcal{L}$

where we used (3.37). By re-arranging the terms in the triple product, we have

$$m = \frac{1}{4\pi} \oint_{\mathcal{C}} \oint_{\mathcal{L}} \frac{(\boldsymbol{x} - \boldsymbol{x}^*) \cdot \mathrm{d}\boldsymbol{l}(\boldsymbol{x}) \times \mathrm{d}\boldsymbol{l}(\boldsymbol{x}^*)}{|\boldsymbol{x} - \boldsymbol{x}^*|^3} , \tag{3.40}$$

which defines the *linking number* $Lk(\mathcal{C}, \mathcal{L})$ of $\mathcal{C}$ and $\mathcal{L}$. This is a fundamental invariant of low-dimensional topology, and it was introduced by Gauss (without derivation and any reference to physics) in 1833, to denote the topological property of two closed curves linked in space. A derivation of Gauss' formula was provided by Maxwell (in the second volume of his *Treatise*, 1873), who made use of the solid angle interpretation of the magnetic potential, as pointed out at the end of Sect. 3.3.1 (for a historical reconstruction and derivation, see [25]).

3.4 The Impact of Topology on Physics: The Aharonov-Bohm Effect

In an influential paper Aharonov and Bohm [1] proposed an experiment to demonstrate that topology has a measurable effect in physics. In their proposal they consider a flow of electrons in a region of space where a magnetic flux tube is present. The magnetic field $\boldsymbol{B}$ is produced by a current carrying solenoid, and it is supposedly confined within the tubular region of the solenoid, so that no measurable magnetic field can be detected outside. The flux tube represents an obstruction for the flow of particles, so that the electrons are scattered away, and the field-free ambient space becomes a multiply connected region. In classical mechanics the particle scattering cannot be influenced by the field inside the solenoid, but in the quantum context it is the magnetic vector potential $\boldsymbol{A}$, and not the field $\boldsymbol{B}$, that governs the wavefunction. Since by Stokes' theorem the magnetic flux Φ can be related to the vector potential $\boldsymbol{A}$, Aharonov and Bohm argued that the quantum mechanical scattering governed by the Schrödinger equation does indeed depend on Φ. Their conjecture was initially confirmed by Chambers and others, and conclusively demonstrated by the Tonomura group [29].

To understand this, let us consider Faraday's equation in ideal conditions

$$\frac{\partial \boldsymbol{B}}{\partial t} = -\nabla \times \boldsymbol{E} , \tag{3.41}$$

with $\boldsymbol{B} = \nabla \times \boldsymbol{A}$, and $\boldsymbol{A}$ satisfying the Coulomb gauge condition $\nabla \cdot \boldsymbol{A} = 0$. By uncurling (3.41) we have the equation for the transport of $\boldsymbol{A}$ in terms of the electric field $\boldsymbol{E}$ and the electric scalar potential ϕ_{e}, that is

$$\frac{\partial \boldsymbol{A}}{\partial t} = -\boldsymbol{E} - \nabla \phi_{\mathrm{e}} . \tag{3.42}$$

As we see, $\boldsymbol{E}$ is completely determined by the potentials $\boldsymbol{A}$ and ϕ_{e}, with a degree of arbitrariness in the choice of these potentials; for example, if we modify them by taking

$$\boldsymbol{A} \to \boldsymbol{A}' = \boldsymbol{A} + \nabla\varphi \,, \qquad \phi_{\mathrm{e}} \to \phi_{\mathrm{e}}' = \phi_{\mathrm{e}} - \partial_t \varphi \,, \tag{3.43}$$

where $\varphi = \varphi(\boldsymbol{x}, t)$ is a smooth, scalar function of space and time, Eq. (3.41) remains unchanged. These are *gauge transformations* that leave the governing equations unchanged. Indeed, if ψ is the wavefunction of the Schrödinger equation, function of $\boldsymbol{A}$ and ϕ_{e}, the new wavefunction under the gauge transformation (3.43) is given by

$$\psi'(\boldsymbol{x}, t) = \mathrm{e}^{\mathrm{i}\varphi(\boldsymbol{x},t)}\psi(\boldsymbol{x}, t) \,. \tag{3.44}$$

We may notice that the new phase factor has no physical observable consequences, because the only term that appears in the computation of position, momentum, and other physical quantities is $|\psi|^2 = |\psi'|^2$; hence, the governing equation remains unaffected by the gauge change.

In the experiment proposed by Aharonov and Bohm the flow of electrons travels through some empty space where $\boldsymbol{B} = \boldsymbol{0}$, and after passing by the solenoid of magnetic flux Φ (see Fig. 3.11a), hit an interference device (Fig. 3.11b). For the electron and the vector potential, the ambient space is doubly connected due to the presence of the flux tube. By applying Stokes' theorem, we have

$$\Phi = \int_{S_0} \boldsymbol{B} \cdot \mathrm{d}\boldsymbol{S} = \int_{S_0} (\nabla \times \boldsymbol{A}) \cdot \mathrm{d}\boldsymbol{S} = \oint_{\mathcal{C}_0} \boldsymbol{A} \cdot \mathrm{d}\boldsymbol{l} \neq 0 \,, \tag{3.45}$$

where $\mathcal{C}_0$ is a loop encircling the flux tube of cross-section S_0.

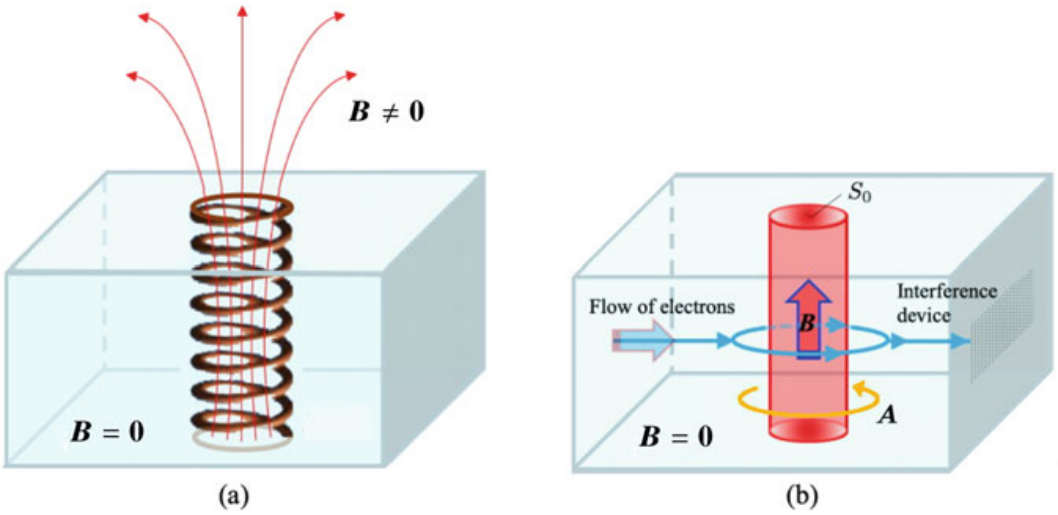

Fig. 3.11 (**a**) A magnetic flux tube is produced by a current carrying solenoid confining the magnetic field $\boldsymbol{B} \neq \boldsymbol{0}$ in its interior. (**b**) A flow of electrons travels in the exterior region (where $\boldsymbol{B} = \boldsymbol{0}$), and after passing by the solenoid hits an interference device

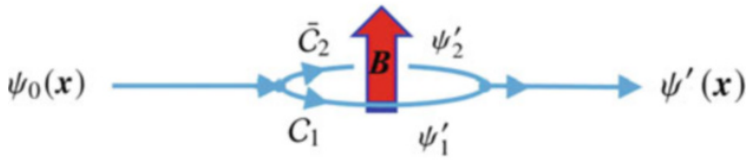

Fig. 3.12 Decomposition of the wavefunction $\psi_0(\boldsymbol{x})$ along the paths $\mathcal{C}_1$ and $\bar{\mathcal{C}}_2$

If the magnetic strength is sufficiently intense, the flow of electrons travels around the solenoid by splitting into two separate beams along the paths $\mathcal{C}_1$ and $\bar{\mathcal{C}}_2$. The particles' path $\mathcal{C}_0$ can thus be thought of as made of two separate paths $\mathcal{C}_1$ and $\mathcal{C}_2$, with $\mathcal{C}_0 = \mathcal{C}_1 \cup \mathcal{C}_2$ oriented according to the right-hand rule given by the direction of the vector potential $\boldsymbol{A}$; let $\bar{\mathcal{C}}_2$ denote the oppositely oriented arc $\mathcal{C}_2$ (see Fig. 3.12). Consider the gauge transformation $\boldsymbol{A}_0 = \boldsymbol{A} - \nabla\varphi = \boldsymbol{0}$ that gives $\boldsymbol{B} = \boldsymbol{0}$ in the region exterior to the solenoid, and let ψ_0 be the wave function that satisfies the Schrödinger equation in terms of this $\boldsymbol{A}_0$. The incident wavefunction ψ_0 gets split into the wavefunctions that govern the two separate beams along $\mathcal{C}_1$ and $\bar{\mathcal{C}}_2$. If ψ' denote the emerging wavefunction, according to (3.44) we have the time independent transformation

$$\psi'(\boldsymbol{x}) = \mathrm{e}^{\mathrm{i}\varphi(\boldsymbol{x})}\psi_0(\boldsymbol{x}) \,, \tag{3.46}$$

so that the resulting wavefunction ψ' is given by the superposition of ψ_1' and ψ_2' for the two electron beams along $\mathcal{C}_1$ and $\bar{\mathcal{C}}_2$; by combining the last integral of (3.45) with (3.46), we have

$$\psi_1'(\boldsymbol{x}) = \mathrm{e}^{\,\mathrm{i}\int_{\mathcal{C}_1}\mathbf{A}\cdot\mathrm{d}\boldsymbol{l}}\,\psi_1(\boldsymbol{x}) \,, \qquad \psi_2'(\boldsymbol{x}) = \mathrm{e}^{\,\mathrm{i}\int_{\bar{\mathcal{C}}_2}\mathbf{A}\cdot\mathrm{d}\boldsymbol{l}}\,\psi_2(\boldsymbol{x}) \,, \tag{3.47}$$

where ψ_1 and ψ_2 are the corresponding incident wavefunctions.

By linear superposition of the two states, we have:

$$\begin{aligned}
\psi_1'(\boldsymbol{x}) + \psi_2'(\boldsymbol{x}) &= \mathrm{e}^{\,\mathrm{i}\int_{\mathcal{C}_1}\mathbf{A}\cdot\mathrm{d}\boldsymbol{l}}\,\psi_1(\boldsymbol{x}) + \mathrm{e}^{\,\mathrm{i}\int_{\bar{\mathcal{C}}_2}\mathbf{A}\cdot\mathrm{d}\boldsymbol{l}}\,\psi_2(\boldsymbol{x}) \\
&= \left[\mathrm{e}^{\,\mathrm{i}\left(\int_{\mathcal{C}_1}\mathbf{A}\cdot\mathrm{d}\boldsymbol{l} - \int_{\bar{\mathcal{C}}_2}\mathbf{A}\cdot\mathrm{d}\boldsymbol{l}\right)}\psi_1(\boldsymbol{x}) + \psi_2(\boldsymbol{x})\right]\mathrm{e}^{\,\mathrm{i}\int_{\bar{\mathcal{C}}_2}\mathbf{A}\cdot\mathrm{d}\boldsymbol{l}} \\
&= \left[\mathrm{e}^{\,\mathrm{i}\left(\int_{\mathcal{C}_1}\mathbf{A}\cdot\mathrm{d}\boldsymbol{l} + \int_{\mathcal{C}_2}\mathbf{A}\cdot\mathrm{d}\boldsymbol{l}\right)}\psi_1(\boldsymbol{x}) + \psi_2(\boldsymbol{x})\right]\mathrm{e}^{\,\mathrm{i}\int_{\bar{\mathcal{C}}_2}\mathbf{A}\cdot\mathrm{d}\boldsymbol{l}} \\
&= \left[\mathrm{e}^{\,\mathrm{i}\oint_{\mathcal{C}_0}\mathbf{A}\cdot\mathrm{d}\boldsymbol{l}}\,\psi_1(\boldsymbol{x}) + \psi_2(\boldsymbol{x})\right]\mathrm{e}^{\,\mathrm{i}\int_{\bar{\mathcal{C}}_2}\mathbf{A}\cdot\mathrm{d}\boldsymbol{l}} \\
&= \left[e^{\mathrm{i}\Phi}\psi_1(\boldsymbol{x}) + \psi_2(\boldsymbol{x})\right]e^{\,\mathrm{i}\int_{\bar{\mathcal{C}}_2}\mathbf{A}\cdot\mathrm{d}\boldsymbol{l}} \,.
\end{aligned}$$

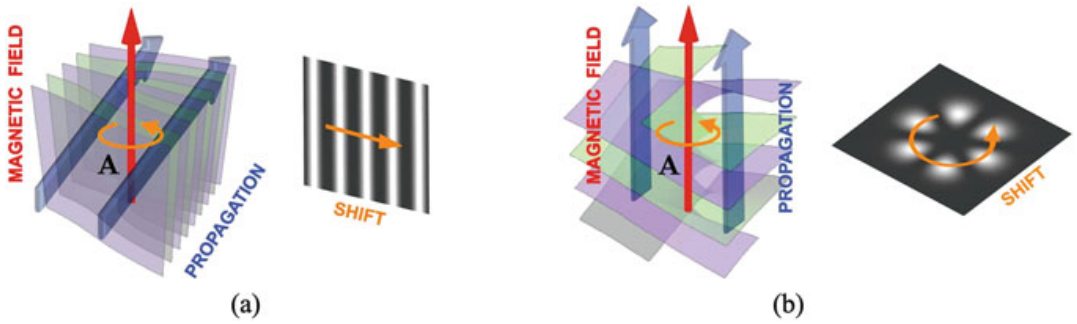

Fig. 3.13 (**a**) The electron wave propagates orthogonally to the magnetic field producing an edge wavefront dislocation; a field-induced transport produces a shift of the interference fringes in the direction orthogonal to both the magnetic field and the propagation of the electrons. (**b**) When the propagation of the electron waves is along the magnetic field the wave fronts carry a screw dislocation (adapted from [11])

We can thus relate the amplitude of the emerging wavefunctions in terms of the incident wavefunctions, so that a change in the flux Φ induces a change in $|\psi_1' + \psi_2'|$. Since the electron flux is coherent (because it is produced by a single source), the difference in amplitude between final and initial wavefunction produces a dislocation of the phase fronts visualised by an interference pattern.

Different orientations of the electron wave propagation and magnetic field produce different effects. In Fig. 3.13a it is shown the transversal dislocation of the interference fringes as expected from the standard Aharonov-Bohm experiment. When the propagation of the electron wave fronts is aligned with the magnetic field (as in Fig. 3.13b) the wave fronts carry a screw dislocation, where the field-induced transport is due to a radial Aharonov-Bohm effect (as shown by [11]).

3.5 Helicity in Multiply Connected Domains

Helicity is a conserved quantity of ideal fluid mechanics and magnetohydrodynamics. In the magnetic context, we have:

Definition 3.3 The *magnetic helicity* H_m is defined by

$$H_m = \int_V \boldsymbol{A} \cdot \boldsymbol{B} \, \mathrm{d}V \ , \tag{3.48}$$

where $\boldsymbol{B} = \nabla \times \boldsymbol{A}$ (with $\nabla \cdot \boldsymbol{A} = 0$) is the magnetic field in the magnetic volume V, such that $\boldsymbol{B} \cdot \hat{\boldsymbol{\nu}} = 0$ on S, where $S = \partial V$ is a magnetic surface of unit normal $\hat{\boldsymbol{\nu}}$.

A similar definition holds for kinetic helicity, replacing $\boldsymbol{B}$ with the vorticity field $\boldsymbol{\omega} = \nabla \times \boldsymbol{u}$, and $\boldsymbol{A}$ with the fluid velocity $\boldsymbol{u}$. Proof of the invariance of the magnetic helicity in ideal magnetohydrodynamics was given by Woltjer [30], and proof of the invariance of the kinetic helicity in the Euler context was provided by Moreau

[24]. When the magnetic field is localised in flux tubes, helicity measures the degree of linking between flux tubes (as anticipated in a footnote by Moreau). A rigorous proof of its interpretation in terms of (Gauss) linking number was provided by the seminal paper of Moffatt [22], followed by the work of Berger and Field [7], and Moffatt and Ricca [23], who showed that helicity can be expressed in terms of the self-linking number. If the magnetic fields are localised in N tubular knots and links, one can prove the following result:

Theorem 3.4 (Moffatt [22]; Moffatt and Ricca [23]) *In ideal conditions the magnetic helicity H_m of N magnetic knots and links, each carrying a magnetic flux Φ_i $(i = 1, \ldots, N)$, is given by*

$$H_m = \int_V \boldsymbol{A} \cdot \boldsymbol{B} \, \mathrm{d}V = \sum_i \Phi_i^2 Sl_i + \sum_{i \neq j} \Phi_i \Phi_j Lk_{ij} \ , \tag{3.49}$$

where Sl_i denotes the (Călugăreanu-White) self-linking number of the i-th magnetic knot, and Lk_{ij} the (Gauss) linking number of the link component i with j.

In simply-connected domains Eq. (3.48) is known to be gauge invariant, but in a multiply connected domain with g holes the original definition of helicity needs a correction to make it gauge invariant. When the ambient space is topologically equivalent to the solid torus ($g = 1$), Moreau demonstrated that this quantity is still conserved, but he didn't consider the implications for a multi-valued potential. The question of having a gauge invariant helicity in a multiply connected domain was addressed recently by MacTaggart and Valli [20], who extended previous work done by Bevir and Gray [8]. Here we reproduce their derivation showing that the use of modern homological concepts provides a mathematical context essentially equivalent to the physical description presented in Sect. 3.2.

For this, let us first recall the Helmholtz decomposition of a vector field [10]:

Theorem 3.5 (Helmholtz's Decomposition) *A vector field $\boldsymbol{u}$ of finite energy, defined on a multiply connected manifold $\mathcal{M}$, admits the following decomposition:*

$$\boldsymbol{u} = \boldsymbol{h} + \nabla\phi + \nabla \times \boldsymbol{f} \ , \tag{3.50}$$

where $\boldsymbol{h}$ is a harmonic field such that $\boldsymbol{u} \cdot \hat{\boldsymbol{\nu}} = 0$ on $S \equiv \partial\mathcal{M}$, ϕ a single-valued scalar field, and $\boldsymbol{f}$ a vector field.

Consider two different vector potentials of $\boldsymbol{B}$, say $\boldsymbol{A}_1$ and $\boldsymbol{A}_2$; since $\nabla \times (\boldsymbol{A}_1 - \boldsymbol{A}_2) = \boldsymbol{0}$, by direct application of Helmholtz's theorem we can write

$$\boldsymbol{A}_1 - \boldsymbol{A}_2 = \boldsymbol{h} + \nabla\chi \ , \tag{3.51}$$

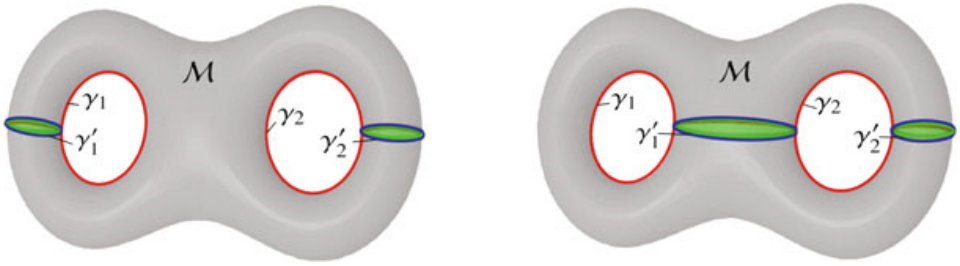

Fig. 3.14 Two different ways to reduce a triply connected manifold $\mathcal{M}$ to a simple connected one through the insertion of two cut surfaces Σ_1 and Σ_2, bounded by the cycles γ_1' and γ_2'

where χ is a scalar function. Let $\tilde{H}_m$ denote the gauge invariant helicity on $\mathcal{M}$, and take the helicity difference given by

$$\begin{aligned}\tilde{H}_{m1} - \tilde{H}_{m2} &= \int_V (\boldsymbol{A}_1 - \boldsymbol{A}_2) \cdot \boldsymbol{B}\, \mathrm{d}V = \int_V (\boldsymbol{A}_1 - \boldsymbol{A}_2) \cdot \boldsymbol{\nabla} \times \boldsymbol{A}_1\, \mathrm{d}V \\ &= \int_S (\boldsymbol{A}_2 - \boldsymbol{A}_1) \cdot \boldsymbol{A}_1 \times \mathrm{d}\boldsymbol{S} = \int_S \boldsymbol{A}_2 \cdot \boldsymbol{A}_1 \times \mathrm{d}\boldsymbol{S}\,; \end{aligned} \tag{3.52}$$

here we used integration by parts, where V denotes the volume of $\mathcal{M}$, and S the bounding surface ($\mathrm{d}\boldsymbol{S} = \mathrm{d}S\hat{\boldsymbol{\nu}}$, with $\hat{\boldsymbol{\nu}}$ unit normal to $S = \partial\mathcal{M}$). According to [20], one can prove that

$$\int_S \boldsymbol{A}_2 \cdot \boldsymbol{A}_1 \times \mathrm{d}\boldsymbol{S} = \sum_{j=1}^{g} \alpha_{1j}\beta_{2j} - \sum_{j=1}^{g} \alpha_{2j}\beta_{1j}\,, \tag{3.53}$$

where g is the number of holes on $\mathcal{M}$ (for the case $g = 2$, see Fig. 3.14),

$$\alpha_{ij} = \oint_{\gamma_j} \boldsymbol{A}_i \cdot \mathrm{d}\boldsymbol{l}_j\,, \qquad \beta_{ij} = \oint_{\gamma_j'} \boldsymbol{A}_i \cdot \mathrm{d}\boldsymbol{l}_j \qquad (i = 1, 2)\,, \tag{3.54}$$

$\gamma_j' = \partial\Sigma_j$ denoting the boundary curve of the cut surface Σ_j ($j = 1, \ldots, g$), γ_j the corresponding co-cycle, and $\{\gamma_j'\}_{j=1}^{g} \cup \{\gamma_j\}_{j=1}^{g}$ the generators of the first homology group of $\partial\mathcal{M}$. Using Stokes' theorem, we have

$$\beta_{ij} = \oint_{\gamma_j'} \boldsymbol{A}_i \cdot \mathrm{d}\boldsymbol{l}_j = \int_{\Sigma_j} \boldsymbol{\nabla} \times \boldsymbol{A}_i \cdot \mathrm{d}\boldsymbol{S}_j = \int_{\Sigma_j} \boldsymbol{B} \cdot \mathrm{d}\boldsymbol{S}_j\,. \tag{3.55}$$

Combining Eq. (3.52) with (3.53) and (3.55), we have

$$\tilde{H}_{m1} - \tilde{H}_{m2} = \sum_{j=1}^{g} \Big[\oint_{\gamma_j} (\boldsymbol{A}_1 - \boldsymbol{A}_2) \cdot \mathrm{d}\boldsymbol{l}_j \Big] \Big(\int_{\Sigma_j} \boldsymbol{B} \cdot \mathrm{d}\boldsymbol{S}_j \Big)\,. \tag{3.56}$$

The gauge invariant form of the helicity on a multiply connected manifold $\mathcal{M}$ with g holes, is thus given by

$$\tilde{H}_m = \int_V \boldsymbol{A} \cdot \boldsymbol{B} \, \mathrm{d}V - \sum_{j=1}^{g} \oint_{\gamma_j} \boldsymbol{A} \cdot \mathrm{d}\boldsymbol{l}_j \int_{\Sigma_j} \boldsymbol{B} \cdot \mathrm{d}\boldsymbol{S}_j$$

$$= H_m - \sum_{j=1}^{g} \kappa_j \int_{\Sigma_j} \boldsymbol{B} \cdot \mathrm{d}\boldsymbol{S}_j \, , \tag{3.57}$$

where κ_j represents the "circulatory constant" associated with the j-th hole present on $\mathcal{M}$. Note the formal analogy between the correction term given by the last expression on the right-hand side of Eq. (3.57) and that of Eq. (3.23); in both cases the summation is extended to the number of holes present on $\mathcal{M}$, and it is performed on the product of the circulatory constant for each loop $\gamma_j = \partial \Sigma_j$ multiplied by the relative flux through Σ_j.

3.6 Kleinert's Multi-Valued Gauge Theory for Singular Fields

In this section we want to show an application of Kleinert's [19] multi-valued gauge theory of currents to provide a fluid dynamical description of a vortex defect in a condensate [31]. Since the defect is an empty tubular region in a fluid domain, the ambient space is no longer simply connected. To reduce the doubly connected region to simple connectivity we can apply Kleinert's technique (see [19, Sec. 4.2], and [13]) by inserting a cut surface. Let us identify a vortex defect with a nodal line $\mathcal{L}$ of the wavefunction, governed by the Gross-Pitaevskii mean field equation. This line can be viewed as the locus of intersection of a fan of surfaces S of constant phase χ (*isophase*) hinged on $\mathcal{L}$, where we identify χ with the polar angle θ (see Fig. 3.15).

By exploiting the hydrodynamic formulation of the Gross-Pitaevskii equation [5], particles motion is governed by a fluid velocity $\boldsymbol{u} = (\hbar/m)\nabla\chi$ normal to the isophase surface S (where $\hbar/m$ is the reduced Planck constant per unit of mass), where χ plays the role of a kinetic potential. In this context, in analogy with a current-carrying loop, the velocity induced by a vortex defect on $\mathcal{L}$ is given by the Biot-Savart induction law. From (3.35), by replacing $\boldsymbol{B}$ with $\boldsymbol{u}$ and I with the vortex circulation Γ, we can compute the velocity in terms of the solid angle, i.e.

$$\boldsymbol{u}(\boldsymbol{x}) = \frac{\Gamma}{4\pi} \nabla\Omega(\boldsymbol{x}) \, . \tag{3.58}$$

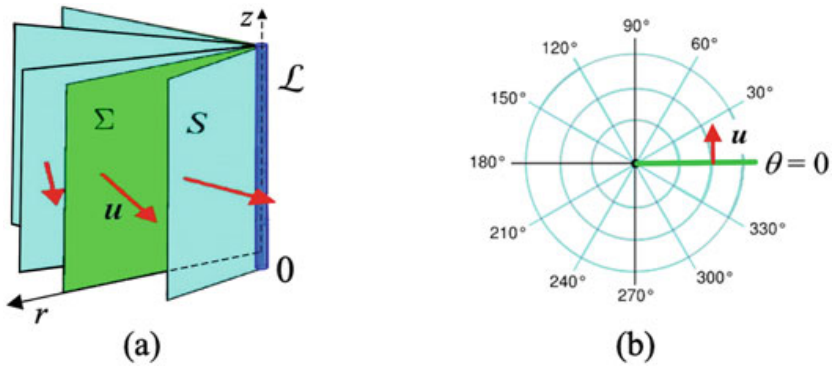

Fig. 3.15 (**a**) A defect $\mathcal{L}$ (visualised by the thin tube along the z-axis) is given by a nodal line of the wavefunction. It can be seen as the locus of intersections of infinitely many surfaces S of constant phase χ, hinged on $\mathcal{L}$; a cut surface Σ can be identified with one of such isophase surfaces. (**b**) In the (xy)-plane the phase χ is identified by the polar angle θ, and the corresponding cut is given by the highlighted segment at $\theta = 0$. The arrow denotes the velocity $\boldsymbol{u} \propto \boldsymbol{\nabla}\chi$

The vorticity $\boldsymbol{\omega} = \boldsymbol{\nabla} \times \boldsymbol{u}$ is a singular field on $\mathcal{L}$, that is

$$\boldsymbol{\omega}(\boldsymbol{x}) \equiv \boldsymbol{\delta}_{\mathcal{L}}(\boldsymbol{x}) = \int_{\mathcal{L}} \delta^{(3)}(\boldsymbol{x} - \boldsymbol{x}^*)\, \mathrm{d}\boldsymbol{l} = \delta_{\mathcal{L}}(\boldsymbol{x})\, \hat{\boldsymbol{t}}\,, \tag{3.59}$$

where $\boldsymbol{x}^* \in \mathcal{L}$ denotes a source point, and $\hat{\boldsymbol{t}}$ the unit tangent to $\mathcal{L}$. By applying Stokes' theorem, we can relate $\boldsymbol{\delta}_{\mathcal{L}}(\boldsymbol{x})$ to a singular Dirac delta distribution over an isophase surfaces S hinged on $\mathcal{L}$, i.e. (cf. [19], eq. 4.24)

$$\boldsymbol{\delta}_{\mathcal{L}}(\boldsymbol{x}) = \oint_{\mathcal{L}} \delta^{(3)}(\boldsymbol{x} - \boldsymbol{x}^*)\, \mathrm{d}\boldsymbol{l} = \int_S \epsilon_{lmn} \partial_l \delta_m(\boldsymbol{x} - \boldsymbol{x}^*)\, \mathrm{d}S_n = \boldsymbol{\nabla} \times \boldsymbol{\delta}_S(\boldsymbol{x})\,. \tag{3.60}$$

To resolve the multi-valuedness of χ, and the apparent paradox due to the fact that vorticity $\boldsymbol{\omega} = \boldsymbol{\nabla} \times \boldsymbol{u} \propto \boldsymbol{\nabla} \times \boldsymbol{\nabla}\chi = \boldsymbol{0}$, we reduce the fluid domain to simple connectivity by inserting a cut surface Σ. For this we can identify Σ with an isophase surface S, so that $\mathcal{L} = \partial\Sigma$. Using (3.60), we can give Σ a physical meaning by taking $\boldsymbol{\delta}_{\mathcal{L}}(\boldsymbol{x}) = \boldsymbol{\nabla} \times \boldsymbol{\delta}_{\Sigma}(\boldsymbol{x})$, where

$$\boldsymbol{\delta}_{\Sigma}(\boldsymbol{x}) = \int_{\Sigma} \delta^{(3)}(\boldsymbol{x} - \boldsymbol{x}^*)\, \mathrm{d}\boldsymbol{S}\,. \tag{3.61}$$

Since the presence of the cut surface Σ does not alter the value of the solid angle, we have $\Omega(\boldsymbol{x}) = \Omega_{\Sigma}(\boldsymbol{x})$, where the subscript denotes the presence of the cut surface. Remembering that $\hat{\boldsymbol{r}} = (\boldsymbol{x} - \boldsymbol{x}^*)/|\boldsymbol{x} - \boldsymbol{x}^*|$, and denoting by $\boldsymbol{\nabla}^* = \partial_i^* \hat{\boldsymbol{e}}_i$ the derivatives with respect to $\boldsymbol{x}^*$ ($\hat{\boldsymbol{e}}_i$ unit vector in the i-th direction), we can take $\boldsymbol{\nabla} f(\boldsymbol{x} - \boldsymbol{x}^*) = -\boldsymbol{\nabla}^* f(\boldsymbol{x} - \boldsymbol{x}^*)$ and write

$$-\boldsymbol{\nabla}\Omega_{\Sigma}(\boldsymbol{x}) = -\boldsymbol{\nabla} \int_{\Sigma} \left(\frac{\hat{\boldsymbol{r}} \cdot \mathrm{d}\boldsymbol{S}}{r^2} \right) = \int_{\Sigma} \hat{\boldsymbol{e}}_i\, \partial_i^* \left(\frac{r_j}{r^3} \right) \mathrm{d}S_j\,, \tag{3.62}$$

where repeated indices stand for summation. By summing and subtracting the same term, we have

$$
\begin{aligned}
-\nabla\Omega_\Sigma(\boldsymbol{x}) &= \hat{\boldsymbol{e}}_i \int_\Sigma \left[\partial_i^*\left(\frac{r_j}{r^3}\right) \mathrm{d}S_j - \partial_j^*\left(\frac{r_j}{r^3}\right) \mathrm{d}S_i\right] + \hat{\boldsymbol{e}}_i \int_\Sigma \partial_j^*\left(\frac{r_j}{r^3}\right) \mathrm{d}S_i \\
&= -\hat{\boldsymbol{e}}_i \int_\Sigma (\mathrm{d}S_j \partial_i - \mathrm{d}S_i \partial_j)\frac{r_j}{r^3} - \int_\Sigma \partial_j\left(\frac{r_j}{r^3}\right) \mathrm{d}\boldsymbol{S} \,. \qquad (3.63)
\end{aligned}
$$

The surface integral above can be converted to a line integral by Stokes' theorem

$$
\int_\Sigma \nabla \times \boldsymbol{f} \cdot \mathrm{d}\boldsymbol{S} = \oint_{\partial\Sigma} \boldsymbol{f} \cdot \mathrm{d}\boldsymbol{l} \,, \qquad (3.64)
$$

where $\boldsymbol{f} = f_q \hat{\boldsymbol{e}}_q$ denotes a generic vector field in $\mathbb{R}^3$. In index notation this is given by

$$
\int_\Sigma \epsilon_{ijk}\partial_i f_j \mathrm{d}S_k = \int_\Sigma \epsilon_{kij}\mathrm{d}S_k \partial_i f_j = \int_\Sigma (\mathrm{d}\boldsymbol{S} \times \nabla) \cdot \boldsymbol{f} = \oint_{\partial\Sigma} f_q \mathrm{d}l_q = \oint_{\partial\Sigma} \boldsymbol{f} \cdot \mathrm{d}\boldsymbol{l} \,. \qquad (3.65)
$$

Let us apply (3.64) to the special case $\boldsymbol{f} = (1/r)\sum_{q=1}^{3} \hat{\boldsymbol{e}}_q$ (taking $f_1 = f_2 = f_3 = 1/r$); we have

$$
\int_\Sigma (\mathrm{d}\boldsymbol{S} \times \nabla) \cdot \frac{1}{r}\sum_{q=1}^{3} \hat{\boldsymbol{e}}_q = \oint_{\partial\Sigma} \frac{1}{r}\Big(\sum_{q=1}^{3} \hat{\boldsymbol{e}}_q\Big) \cdot \mathrm{d}\boldsymbol{l} \,. \qquad (3.66)
$$

Knowing that $\hat{\boldsymbol{e}}_p \cdot \hat{\boldsymbol{e}}_q = \delta_{pq}$, the surface integral above becomes

$$
\int_\Sigma \frac{1}{2}\hat{\boldsymbol{e}}_p \epsilon_{pji}(\mathrm{d}S_j \partial_i - \mathrm{d}S_i \partial_j)\frac{1}{r}\sum_{q=1}^{3} \hat{\boldsymbol{e}}_q = \sum_{q=1}^{3} \int_\Sigma \frac{1}{2}\epsilon_{qji}(\mathrm{d}S_j \partial_i - \mathrm{d}S_i \partial_j)\frac{1}{r} \,; \qquad (3.67)
$$

by equating (3.67) with the right-hand side of (3.66), we have

$$
\int_\Sigma (\mathrm{d}S_j \partial_i - \mathrm{d}S_i \partial_j)\frac{1}{r} = \epsilon_{kji} \oint_{\partial\Sigma} \frac{1}{r}\mathrm{d}l_k \,. \qquad (3.68)
$$

Let us consider now the first integral on the right-hand side of Eq. (3.63), and rewrite it as follows:

$$
\begin{aligned}
-\hat{\boldsymbol{e}}_i \int_\Sigma (\mathrm{d}S_j \partial_i - \mathrm{d}S_i \partial_j)\frac{r_j}{r^3} &= \hat{\boldsymbol{e}}_i \int_\Sigma (\mathrm{d}S_j \partial_i - \mathrm{d}S_i \partial_j)\partial_j \frac{1}{r} \\
&= \hat{\boldsymbol{e}}_i \partial_j \int_\Sigma (\mathrm{d}S_j \partial_i - \mathrm{d}S_i \partial_j)\frac{1}{r} \,. \qquad (3.69)
\end{aligned}
$$

Using (3.68), the last term above becomes

$$\hat{\boldsymbol{e}}_i \partial_j \int_\Sigma (\mathrm{d}S_j \partial_i - \mathrm{d}S_i \partial_j) \frac{1}{r} = \hat{\boldsymbol{e}}_i \partial_j \epsilon_{kji} \oint_{\partial\Sigma} \frac{1}{r} \mathrm{d}l_k = \hat{\boldsymbol{e}}_i \oint_{\partial\Sigma} \epsilon_{kji} \left(\partial_j \frac{1}{r}\right) \mathrm{d}l_k$$
$$= -\hat{\boldsymbol{e}}_i \oint_{\partial\Sigma} \epsilon_{kji} \frac{r_j}{r^3} \mathrm{d}l_k = -\oint_{\partial\Sigma} \epsilon_{ikj} \hat{\boldsymbol{e}}_i \mathrm{d}l_k \frac{r_j}{r^3} \,. \quad (3.70)$$

Hence, by combining the left-hand side of (3.69) with the last integral on the right-hand side of (3.70), we have

$$-\hat{\boldsymbol{e}}_i \int_\Sigma (\mathrm{d}S_j \partial_i - \mathrm{d}S_i \partial_j) \frac{r_j}{r^3} = -\oint_{\partial\Sigma} \frac{\mathrm{d}\boldsymbol{l} \times \boldsymbol{r}}{r^3} = -\oint_{\partial\Sigma} \frac{\mathrm{d}\boldsymbol{l} \times \hat{\boldsymbol{r}}}{r^2} \,. \quad (3.71)$$

Consider now the second integral on the right-hand side of (3.63); we have

$$-\int_\Sigma \partial_j \left(\frac{r_j}{r^3}\right) \mathrm{d}\boldsymbol{S} = \int_\Sigma \partial_j \left(\partial_j \frac{1}{r}\right) \mathrm{d}\boldsymbol{S} = \int_\Sigma \nabla^2 \frac{1}{r} \, \mathrm{d}\boldsymbol{S} \,. \quad (3.72)$$

Since the fundamental solution to the Poisson equation in $\mathbb{R}^3$ is given by $\nabla^2(1/r) = -4\pi\delta^{(3)}(\boldsymbol{x} - \boldsymbol{x}^*)$, we have

$$-\int_\Sigma \partial_j \left(\frac{r_j}{r^3}\right) \mathrm{d}\boldsymbol{S} = -4\pi \int_\Sigma \delta^{(3)}(\boldsymbol{x} - \boldsymbol{x}^*) \, \mathrm{d}\boldsymbol{S} = -4\pi \boldsymbol{\delta}_\Sigma(\boldsymbol{x}) \,. \quad (3.73)$$

By substituting (3.71) and (3.73) into (3.63), we have

$$-\nabla \Omega_\Sigma(\boldsymbol{x}) = -\oint_{\partial\Sigma} \frac{\mathrm{d}\boldsymbol{l} \times \hat{\boldsymbol{r}}}{r^2} - 4\pi \boldsymbol{\delta}_\Sigma(\boldsymbol{x}) \,; \quad (3.74)$$

thus, using (3.58), the correct expression for the velocity is given by

$$\boldsymbol{u}(\boldsymbol{x}) = \frac{\Gamma}{4\pi} \Big[\oint_{\mathcal{L}} \frac{\mathrm{d}\boldsymbol{l} \times \hat{\boldsymbol{r}}}{r^2} + 4\pi \boldsymbol{\delta}_\Sigma(\boldsymbol{x}) \Big] \,. \quad (3.75)$$

The first term on the right-hand side is the classical contribution due to the Biot-Savart induction law, while the second term represents the induction due to the presence of a singular source field on Σ. With reference to the kinetic potential χ, we now have

$$\boldsymbol{\omega} = \nabla \times \boldsymbol{u} \propto \nabla \times [\nabla \chi + \boldsymbol{\delta}_\Sigma(\boldsymbol{x})] = \boldsymbol{\delta}_{\mathcal{L}}(\boldsymbol{x}) \quad (3.76)$$

This demonstrates that Kleinert's technique can be usefully extended and applied to several problems that involve not only multiply connected domains, but also the presence of singular structures, such as vortex sheets in fluid mechanics [6], and current sheets in magnetohydrodynamics [9].

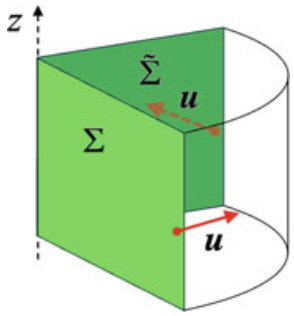

Fig. 3.16 The volume $\tilde{V}$ is given by the cylindrical sector delimited by the two cut surfaces Σ and $\tilde{\Sigma}$, the bottom and top planes z_0 and z_1 constant, and the cylindrical surface (transparent). The two arrows denote the velocity field $\boldsymbol{u} \propto \nabla\chi$ normal to the two cut surfaces

3.6.1 Gauge Invariance of Cut Surfaces

The velocity field given by (3.76) is a gauge invariant quantity, independent evidently of the particular choice of the cut surface Σ ([19], p. 115). Let us demonstrate this by taking a second cut surface $\tilde{\Sigma}$, different from the former; consider the volume of the cylindrical sector delimited by Σ and $\tilde{\Sigma}$ as in Fig. 3.16. Let $\partial\tilde{V} = \Sigma \cup \tilde{\Sigma} \cup \Sigma_0$ be the boundary of $\tilde{V}$ (where Σ_0 denotes the remaining bounding surface given by the top, bottom and cylindrical surface). With reference to the new surface (remembering that the bounding surface $\partial\tilde{V}$ has unit normal $\hat{\boldsymbol{\nu}}$ pointing outwardly), we have

$$\int_{\partial\tilde{V}} \delta^{(3)}(\boldsymbol{x}-\boldsymbol{x}^*)\,\mathrm{d}\boldsymbol{S} = -\int_{\Sigma} \delta^{(3)}(\boldsymbol{x}-\boldsymbol{x}^*)\,\mathrm{d}\boldsymbol{S} + \int_{\tilde{\Sigma}} \delta^{(3)}(\boldsymbol{x}-\boldsymbol{x}^*)\,\mathrm{d}\boldsymbol{S} + \int_{\Sigma_0} \delta^{(3)}(\boldsymbol{x}-\boldsymbol{x}^*)\,\mathrm{d}\boldsymbol{S}\,; \tag{3.77}$$

the contribution from the last integral is zero, because there is no flux through Σ_0. Hence

$$\boldsymbol{\delta}_{\tilde{\Sigma}}(\boldsymbol{x}) = \int_{\tilde{\Sigma}} \delta^{(3)}(\boldsymbol{x}-\boldsymbol{x}^*)\,\mathrm{d}\boldsymbol{S} = \int_{\Sigma} \delta^{(3)}(\boldsymbol{x}-\boldsymbol{x}^*)\,\mathrm{d}\boldsymbol{S} + \int_{\partial\tilde{V}} \delta^{(3)}(\boldsymbol{x}-\boldsymbol{x}^*)\,\mathrm{d}\boldsymbol{S}\,. \tag{3.78}$$

Now, let's apply the generalised Stokes' theorem to the last integral. Consider an arbitrary, constant vector field $\hat{\boldsymbol{e}}$ fixed in space. Using the divergence theorem, we have

$$\begin{aligned}
\hat{\boldsymbol{e}} \cdot \int_{\partial\tilde{V}} \delta^{(3)}(\boldsymbol{x}-\boldsymbol{x}^*)\,\mathrm{d}\boldsymbol{S} &= \int_{\partial\tilde{V}} \delta^{(3)}(\boldsymbol{x}-\boldsymbol{x}^*)\,\hat{\boldsymbol{e}}\cdot\mathrm{d}\boldsymbol{S} = \int_{\tilde{V}} \nabla^*\cdot[\delta^{(3)}(\boldsymbol{x}-\boldsymbol{x}^*)\,\hat{\boldsymbol{e}}]\,\mathrm{d}V \\
&= \int_{\tilde{V}} [\nabla^*\delta^{(3)}(\boldsymbol{x}-\boldsymbol{x}^*)\cdot\hat{\boldsymbol{e}} + \delta^{(3)}(\boldsymbol{x}-\boldsymbol{x}^*)\nabla^*\cdot\hat{\boldsymbol{e}}]\,\mathrm{d}V \\
&= \hat{\boldsymbol{e}}\cdot\int_{\tilde{V}} \nabla^*\delta^{(3)}(\boldsymbol{x}-\boldsymbol{x}^*)\,\mathrm{d}V = -\hat{\boldsymbol{e}}\cdot\int_{\tilde{V}} \nabla\,\delta^{(3)}(\boldsymbol{x}-\boldsymbol{x}^*)\,\mathrm{d}V\,,
\end{aligned}$$

i.e.

$$\int_{\partial\tilde{V}} \delta^{(3)}(\boldsymbol{x}-\boldsymbol{x}^*)\,\mathrm{d}\boldsymbol{S} = -\int_{\tilde{V}} \boldsymbol{\nabla}\,\delta^{(3)}(\boldsymbol{x}-\boldsymbol{x}^*)\,\mathrm{d}V\ . \tag{3.79}$$

Substituting (3.79) into the right-hand side of (3.78), we have

$$\boldsymbol{\delta}_{\tilde{\Sigma}}(\boldsymbol{x}) = \int_{\Sigma} \delta^{(3)}(\boldsymbol{x}-\boldsymbol{x}^*)\,\mathrm{d}\boldsymbol{S} - \int_{\tilde{V}} \boldsymbol{\nabla}\,\delta^{(3)}(\boldsymbol{x}-\boldsymbol{x}^*)\,\mathrm{d}V\ , \tag{3.80}$$

that is

$$\boldsymbol{\delta}_{\tilde{\Sigma}}(\boldsymbol{x}) = \boldsymbol{\delta}_{\Sigma}(\boldsymbol{x}) - \boldsymbol{\nabla}\,\delta^{(3)}(\boldsymbol{x}-\boldsymbol{x}^*)\ . \tag{3.81}$$

Thus, taking the curl we have

$$\boldsymbol{\nabla}\times\boldsymbol{\delta}_{\Sigma}(\boldsymbol{x}) = \boldsymbol{\nabla}\times\boldsymbol{\delta}_{\tilde{\Sigma}}(\boldsymbol{x})\ , \tag{3.82}$$

which proves the gauge invariance of (3.76).

The change of gauge involves also a change of the phase. By the solid angle interpretation of χ, and by applying again the generalised Stokes theorem, we have

$$\begin{aligned}\chi_{\tilde{\Sigma}}(\boldsymbol{x}) &= \int_{\tilde{\Sigma}} \frac{\hat{\boldsymbol{r}}\cdot\mathrm{d}\boldsymbol{S}}{r^2} = \int_{\Sigma} \frac{\hat{\boldsymbol{r}}\cdot\mathrm{d}\boldsymbol{S}}{r^2} + \int_{\Delta\Sigma} \frac{\hat{\boldsymbol{r}}\cdot\mathrm{d}\boldsymbol{S}}{r^2} \\ &= \chi_{\Sigma}(\boldsymbol{x}) - \int_{\Delta\Sigma} \boldsymbol{\nabla}\Big(\frac{1}{r}\Big)\cdot\mathrm{d}\boldsymbol{S} = \chi_{\Sigma}(\boldsymbol{x}) - \int_{\tilde{V}} \nabla^2\Big(\frac{1}{r}\Big)\,\mathrm{d}V\ .\end{aligned} \tag{3.83}$$

Using $\nabla^2(1/r) = -4\pi\,\delta^{(3)}(\boldsymbol{x}-\boldsymbol{x}^*)$, Eq. (3.83) reduces to

$$\chi_{\tilde{\Sigma}}(\boldsymbol{x}) = \chi_{\Sigma}(\boldsymbol{x}) + 4\pi\,\delta^{(3)}(\boldsymbol{x}-\boldsymbol{x}^*)\ , \tag{3.84}$$

which shows the stated phase change. Note that by taking the gradient

$$\boldsymbol{\nabla}\chi_{\Sigma}(\boldsymbol{x}) = \boldsymbol{\nabla}\chi_{\tilde{\Sigma}}(\boldsymbol{x}) + \boldsymbol{\nabla}\delta^{(3)}(\boldsymbol{x}-\boldsymbol{x}^*)\ ; \tag{3.85}$$

and substituting this equation into (3.76), the value of the velocity remains unaffected.

3.6.2 *Application of Kleinert's Theory to a Circular, Singular Current*

As mentioned, Kleinert's technique is of general validity, and it can be applied to several problems that involve singular vector fields. As an example consider the

classical problem of determining the magnetic field $\boldsymbol{B}$ induced by a circular, current-carrying wire $\mathcal{L}_0$, of radius R and current intensity I. Let the wire be placed in the (xy)-plane, centred at the origin of the reference system $\{\hat{\boldsymbol{i}}, \hat{\boldsymbol{j}}, \hat{\boldsymbol{k}}\}$; we want to determine the induced field at a generic point $\boldsymbol{x}$ along the z-axis. Let $r = |\boldsymbol{x} - \boldsymbol{x}^*|$ denote the distance between the induction and the source point at $\boldsymbol{x}^* \in \mathcal{L}_0$. The solid angle Ω subtended by the loop wire at the observation point at $\boldsymbol{x}$ is, in general, a multi-valued function. We consider two cases: (i) $\Omega = \Omega_\Sigma(\boldsymbol{x})$ single-valued by the presence of a cut-surface Σ, and (ii) $\Omega = \Omega(\boldsymbol{x})$ multi-valued.

In the first case let us consider the cut-surface Σ given by the circular disk centred at the origin in the (x, y)-plane, with $\mathcal{L}_0 = \partial\Sigma$. Using spherical polar coordinates centred at the origin, we have

$$\mathrm{d}S = r^2 \sin\theta \, \mathrm{d}\theta \, \mathrm{d}\varphi \, . \tag{3.86}$$

By the standard definition of solid angle (see Eq. 3.24), we have

$$\Omega_\Sigma(\boldsymbol{x}) = \int_0^{2\pi} \mathrm{d}\varphi \int_0^{\theta} \frac{r^3 \sin\theta}{r^3} \mathrm{d}\theta = 2\pi(1 - \cos\theta) \, . \tag{3.87}$$

In the second case, one can show [4] that

$$\Omega(\boldsymbol{x}) = \int_S \frac{\hat{\boldsymbol{r}} \cdot \mathrm{d}\boldsymbol{S}}{r^2} = \int_S \nabla \times \left[\frac{\hat{\boldsymbol{k}} \times \hat{\boldsymbol{r}}}{r(1 \mp \hat{\boldsymbol{k}} \cdot \hat{\boldsymbol{r}})} \right] \cdot \mathrm{d}\boldsymbol{S} = \oint_{\mathcal{L}_0} \frac{\hat{\boldsymbol{t}} \cdot (\hat{\boldsymbol{k}} \times \hat{\boldsymbol{r}})}{r(1 \mp \hat{\boldsymbol{k}} \cdot \hat{\boldsymbol{r}})} \, \mathrm{d}s \, , \tag{3.88}$$

where $\mathcal{L}_0 = \partial S$, and $\hat{\boldsymbol{t}}$ denotes the tangent unit vector to $\mathcal{L}_0$. The $\pm$ sign stands for the two viewing directions along z-axis. A physical interpretation of the sign ambiguity stems from the multi-valuedness of the potential $\hat{\boldsymbol{k}} \times \hat{\boldsymbol{r}}/(1 \mp \hat{\boldsymbol{k}} \cdot \hat{\boldsymbol{r}})$ associated with the monopole-type field $\hat{\boldsymbol{r}}/r^2$. Because of the symmetry of the problem, without loss of generality we can consider r and θ constant by taking $\boldsymbol{x}$ fixed on the z-axis; we have

$$\hat{\boldsymbol{r}} = \sin\theta(\cos\varphi \, \hat{\boldsymbol{i}} + \sin\varphi \, \hat{\boldsymbol{j}}) + \cos\theta \, \hat{\boldsymbol{k}} \, , \qquad \mathrm{d}s = r \sin\theta \, \mathrm{d}\varphi \, ;$$

by varying φ, we have $\hat{\boldsymbol{t}} = \mathrm{d}\boldsymbol{r}/\mathrm{d}s = -\sin\varphi \, \hat{\boldsymbol{i}} + \cos\varphi \, \hat{\boldsymbol{j}}$. The solid angle is thus given by

$$\Omega(\boldsymbol{x}) = \int_0^{2\pi} \frac{\pm \sin^2\theta}{1 \mp \cos\theta} \, \mathrm{d}\varphi = \pm 2\pi(1 \pm \cos\theta) \, , \tag{3.89}$$

that shows the multi-valuedness of Ω. When the induced point goes from one side of S to the other side, the value of the solid angle jumps by

$$[\Omega]_-^+ = 2\pi(1 + \cos\theta) - [-2\pi(1 - \cos\theta)] = 4\pi \, . \tag{3.90}$$

Let us compute the solid angle viewed from the points along z-axis: since $\cos\theta = z/r = z/(R^2+z^2)^{1/2}$, we have

$$\Omega(z) = 2\pi\left(1 - \frac{z}{\sqrt{R^2+z^2}}\right). \tag{3.91}$$

By using (3.35) we have

$$B_z = \boldsymbol{B}\cdot\hat{\boldsymbol{k}} = -\frac{I}{4\pi}\nabla_{\hat{\boldsymbol{k}}}\Omega(z) = -\frac{I}{4\pi}\frac{\partial\Omega(z)}{\partial z}\,, \tag{3.92}$$

so that

$$B_z = \frac{I}{4\pi}2\pi\frac{\partial}{\partial z}\left(\frac{z}{\sqrt{R^2+z^2}}\right) = \frac{I\,R^2}{2(R^2+z^2)^{3/2}}\,, \tag{3.93}$$

as expected from the classical theory.

3.7 Conclusions

In this paper we have shown how ideas and techniques introduced by Riemann to tackle problems that involve multi-valued potentials (Sect. 3.1) find modern application in current topics of topological field theory, and fluid mechanics in particular. Lord Kelvin was the first to apply Riemann's cuts to correct Green's identity in the case of multiply-connected regions. His correction formula is here re-derived (Sect. 3.2) to show how its formal structure anticipates a similar correction introduced for the gauge invariance of helicity (Sect. 3.5). Another interesting strand of research is provided by Gauss' solid angle interpretation of the potential, which allows to re-interpret the Biot-Savart induction law, providing a direct connection between the solid angle concept and the linking number formula (Sect. 3.3). The influence of the topology of the ambient space on the physics is discussed in the context of the Aharonov-Bohm experiment (Sect. 3.4), and finally, in Sect. 3.6, we show how Kleinert's multi-valued gauge theory of currents is applied to determine the exact expression for the velocity of a vortex defect in condensates. The methods presented here are of general validity, finding renovated life in the study of new, emergent phenomena in multiply connected domains [12, 14].

Acknowledgments R.L.R. and X.L. wish to acknowledge financial support from the Beijing Natural Science Foundation (grant n. XXXXX, Z180007) and the National Natural Science Foundation of China (grant n. 11572005).

References

1. Aharonov, B., Bohm, D.: Significance of the electromagnetic potentials in the quantum theory. Phys. Rev. **115**, 485–491 (1959)
2. Ahlfors, L., Sario, L.: Riemann Surfaces. Princeton University Press, Princeton (1960)
3. Archibald, T.: Connectivity and smoke-rings: Green's second identity in its first fifty years. Math. Mag. **62**, 219–232 (1989)
4. Asvestas, J.S.: Line integrals and physical optics. Part I. The transformation of the solid-angle surface integral to a line integral. J. Optical Soc. Am. A **2**, 891–895 (1985)
5. Barenghi, C.F., Parker, N.G.: A Primer on Quantum Fluids. Springer, Berlin (2016)
6. Batchelor, G.K.: An Introduction to Fluid Dynamics. Cambridge University Press, Cambridge (2000)
7. Berger, M.A., Field, G.B. The topological properties of magnetic helicity. J. Fluid Mech. **14**, 133–148 (1984)
8. Bevir, M., Gray, J.W.: Relaxation, flux consumption and quasi steady state pinches. Proc. Reversed Field Pinch Theory Workshop LA-8944-C 176–180 (1980)
9. Biskamp, D.: Magnetic Reconnection in Plasmas. Cambridge University Press, Cambridge (2000)
10. Blank, A.A., Friedrichs, K.O., Grad, H.: Notes on magneto-hydrodynamics V. Theory of Maxwell's equations without displacement current. AEC Research and Development Report NYO-6486 (1957)
11. Bliokh, K.Y., Schattschneider, P., Verbeeck, J., Nori, F.: Electron vortex beams in a magnetic field: a new twist on Landau levels and Aharonov-Bohm states. Phys. Rev. X **2**, 041011 (2012)
12. Foresti, M., Ricca, R.L.: Defect production by pure twist induction as Aharonov-Bohm effect. Phys. Rev. E **100**, 023107 (2019)
13. Foresti, M., Ricca, R.L.: Hydrodynamics of a quantum vortex in the presence of twist. J. Fluid Mech. **904**, A25 (2020)
14. Foresti, M., Ricca, R.L.: Instability of a quantum vortex by twist perturbation. J. Fluid Mech. **949**, A19 (2022)
15. Gauss, C.F.: Allgemeine Theorie des Erdmagnetismus. In: Gauss, C.F., Weber, W. (eds.) Resultate aus den Beobachtungen des magnetischen Vereins im Jahre 1838, pp. 1–57. Weidmannsche Buchhandlung, Leipzig (1839)
16. Helmholtz, H.: Über Integrale der hydrodynamischen Gleichungen welche den Wirbelbewegungen entsprechen. J. Math. **55** 25–55 (1858) [For an English translation see: Parpart, U.: On integrals of the hydrodynamic equations that correspond to vortex motions. Int. J. Fusion Energy **1**, 41–68 (1978)]
17. Jackson, J.D.: Classical Electrodynamics. John Wiley & Sons, Inc., Hoboken (1999)
18. Jänich, K.: Topology. Springer-Verlag, Berlin (1984)
19. Kleinert, H.: Multivalued Fields in Condensed Matter, Electromagnetism and Gravitation. World Scientific, Singapore (2008)
20. MacTaggart, D., Valli, A.: Magnetic helicity in multiply connected domains. J. Plasma Phys. **85**, 775850501 (2019)
21. Maxwell, J.C.: A Treatise on Electricity and Magnetism. MacMillan & Co., Oxford (1873)
22. Moffatt, H.K.: The degree of knottedness of tangled vortex lines. J. Fluid Mech. **35**, 117–129 (1969)
23. Moffatt, H.K., Ricca R.L.: Helicity and the Călugăreanu invariant. Proc. R. Soc. Lond. A **439**, 411–429 (1992)
24. Moreau, J.J.: Constantes d'un îlot tourbillonnaire en fluide parfait barotrope. Comptes Rendus Hebdom, Sèances Acad. Sci. **252**, 2810–2812 (1961)
25. Ricca, R.L., Nipoti, B.: Gauss' linking number revisited. J. Knot Theory Its Ramific. **20**, 1325–1343 (2011)

26. Riemann, B.: Lehrsätze aus der analysis situs für die Theorie der Integrale von zweigliedrigen vollständigen Differentialen. J. Mathematik **54**, 105–110 (1857) [For an English translation see: A Source Book in Classical Analysis (ed. G. Birkhoff), pp. 52–56. Harvard U.P. (1973)]
27. Thomson, W. (Lord Kelvin): A mathematical theory of magnetism — continuation of Part I. Philos. Trans. R. Soc. Lond. **June**, 269–285 (1850)
28. Thomson, W. (Lord Kelvin): On vortex motion. Trans. R. Soc. Edin. **25**, 217–260 (1869)
29. Tonomura, A., Osakabe, N., Matsuda, T., Kawasaki, T., Endo, J., Yano, S., Yamada, H.: Evidence for Aharonov-Bohm effect with magnetic field completely shielded from electron wave. Phys. Rev. Lett. **56**, 792–795 (1986)
30. Woltjer, L.: A theorem on force-free magnetic fields. Proc. Natl. Acad. Sci. USA **44**, 489–491 (1958)
31. Wyatt, R.E.: Quantum Dynamics with Trajectories. Springer, New York (2005)